

# **Active deformation of the Shargyn Basin, a transpressional strike-slip intersection in western Mongolia.**

by

Thomas Ben Thompson

Submitted to the Department of Earth, Atmospheric and Planetary Science  
in partial fulfillment of the requirements for the degree of

Bachelor of Science in Earth, Atmospheric and Planetary Sciences

at the

MASSACHUSETTS INSTITUTE OF TECHNOLOGY

June 2013

© Thomas Ben Thompson. All rights reserved.

The author hereby grants to MIT permission to reproduce and to distribute  
publicly paper and electronic copies of this thesis document in whole or in part in  
any medium now known or hereafter created.

Author .....  
Department of Earth, Atmospheric and Planetary Science  
May 10, 2013

Certified by .....  
Oliver Jagoutz  
Assistant Professor  
Thesis Supervisor

Accepted by .....  
Samuel Bowring  
Chair, Committee on Undergraduate Program

# **Active deformation of the Shargyn Basin, a transpressional strike-slip intersection in western Mongolia.**

by

Thomas Ben Thompson

Submitted to the Department of Earth, Atmospheric and Planetary Science  
on May 10, 2013, in partial fulfillment of the  
requirements for the degree of  
Bachelor of Science in Earth, Atmospheric and Planetary Sciences

## **Abstract**

Intraplate faulting in central Asia is a major component of the Indo-Eurasian collision. The kinematics and mechanisms of intraplate deformation are important in understanding broad active tectonic patterns, reconstructing past tectonics, analyzing seismic hazard and identifying potential resources. We examine the fault kinematics surrounding the 150 km wide Shargyn Basin at the intersection of the left-lateral transpressional Gobi-Altai fault system and the right-lateral transpressional Altai fault system. The studies were performed using satellite data and targeted field transects. The results suggest the Shargyn basin is formed by a compressional stepover, an uplifted wedge from the intersecting strike-slip systems and many strike-slip terminating thrust splays. Furthermore, local foliation is almost always fault parallel, pointing to the importance of pre-existing structural weaknesses in the development of active faults. This research demonstrates some of the potential kinematics for intraplate transpressional orogenies and emphasizes the importance of pre-existing crustal structure in the development of active faults.

Thesis Supervisor: Oliver Jagoutz  
Title: Assistant Professor

## Acknowledgments

Primarily, I thank Claire Bucholz (EAPS PhD candidate) for wandering the Mongolian steppes and mountains and teaching me endlessly about geology and EAPS Professor Oliver Jagoutz for supervising and helping me through the whole thesis process. I thank the UROP office and the EAPS department for supporting my field work in Mongolia last summer.

# Contents

1	Motivation . . . . .	8
2	Background on Mongolian Active Deformation . . . . .	9
2.1	Mongolian Deformation in Context – Asia . . . . .	9
2.2	Shargyn Basin . . . . .	13
2.3	Bedrock Geology . . . . .	15
3	Structural Evidence . . . . .	18
3.1	Remote Sensing . . . . .	18
3.2	Field Mapping . . . . .	18
3.3	Khantaishir Thrusts . . . . .	19
3.4	Bogd Fault and Termination Thrust Splays . . . . .	22
3.5	Tonhil Fault and Intersection Wedge Thrusts . . . . .	24
3.6	Shargyn Fault and Termination Thrust Splays . . . . .	25
3.7	Earthquake Mechanisms and Locations . . . . .	30
3.8	Interpretation and Discussion . . . . .	32
4	Conclusion . . . . .	34
1	Appendix A: More cross sections. . . . .	35

# List of Figures

- 1 "Simplified tectonic map of East Asia and the Western Pacific illustrating latest Cretaceous and Cenozoic faults in East Asia. 1, 2 and 3 are major thrust, strike-slip and normal fault, respectively; 4, 5 and 6 are convergent (filled triangles are for active and open triangles are for inactive boundary), transform and divergent plate boundary, respectively; 7 is land; 8 is sea, with dark grey being basin or ocean floor and light grey being continental shelf or morphological high on basin or ocean floor. BHb, Bohaiwan basin; BSb, Banda Sea basin; CKg, Central Kamchatka graben; ECSb, East China Sea basin; FMg, Fushun-Meikehou graben; Fr, Fenwei rift; HYr, Hetao-Yinchuan rift; Jb, Java basins; MGb, Mergui basin; MLb, Malay basin; OT, Okinawa Trough; Pb, Pattani basin; Sb, Sumatra basins; SCSb, South China Sea basin; SCSmb, South China Sea marginal basin; SHdsz, Sakhalin-Hokkaido dextral shear zone; SLb, Shantar-Liziansky basin; SXr, Shanxi rift; Yb, Yunqing basin; YSb, Yellow Sea basin; YYg, Yilan-Yitong graben; Zb, Zengmu basin; Zu, Zenghe uplift" [Schellart and Lister, 2005]. The location of Figure 2 is outlined in Central Asia. . . 10
- 2 Shaded relief map of Mongolia with fault overlays and seismic moment tensor solutions for recorded earthquakes. Important locations or faults are labeled. HTF = Hoh-Serh-Tsagaan-Salaa Fault, BF = Bolnay Fault, BGF = Bogd Fault. The study area and location of Figure 3 is outlined in black. The difference between right-lateral transpressional strike-slip in the Altai Range and left-lateral transpressional strike-slip in the Gobi-Altai is especially important. Modified after Calais [2003] . . . 12

3	Landsat Imagery basemap showing important locations for this study. The large white box surrounding the Shargyn Basin is the new mapping from this study. The white area surrounding the Dariv Range indicates mapping performed by Dijkstra and Brouwer [2006] and as a part of unpublished research by Claire Bucholz. The area surrounding the Sutai Range was mapped by Cunningham et al. [2003]. The small white boxes around the Shargyn Basin show areas that we studied in the field. The red lines are labeled cross-sections that will be discussed in the Structural Evidence section. A GPS vector near the city of Altai is shown in the northeast. Earthquake focal mechanisms in the area are also shown. . . . .	13
4	Schematic diagrams showing faulting and deposition for common transpressional uplifts and basins. . . . .	14
5	Schematic tectonostratigraphic map of Mongolia. The area we studied is located in the outlined box. The Main Mongolian Lineament is the black line passing through our study region. Credit to Windley et al. [2007] . . . . .	16
6	Schematic map of the dominant structural grain in western Mongolia. The study area is boxed for reference. The shaded Junggar Block is mechanically rigid. The Junggar Block may be a trapped block of oceanic crust [Carroll et al., 1990]. The Hangay Block consists of microcontinental fragments that accreted during the early stages of the Central Asian Orogeny. It is not shaded because it is probably not mechanically rigid. Modified after Cunningham [2005] . . . . .	17
7	A map of the Shargyn Basin showing the studied faults and important locations. Slip is indicated by thrust teeth or lateral slip arrows. . . . .	19
8	A northeast-southwest cross-section through the Khantaishir Range and the Khan-taishir Thrusts paired with a Landsat image. Important locations and lithology are noted on the satellite image. . . . .	20
9	Photographs of exposed faults. Field workers are used as scale bars. A) An outcrop of the exposed Upper Khantaishir Thrust from cross-section A-A'. B) An outcrop of the exposed thrust in cross-section X1-X1' . . . . .	21
10	A cross-section through the Haliun Thrust and Butara Thrust paired with a Landsat image. Important locations and lithology are noted on the satellite image. . . . .	23

11	Landsat imagery showing the intersection wedge area at the southwestern corner of the Shargyn Basin. Mapped active faults are shown by solid red lines. Slip sense is shown with thrust teeth or lateral slip arrows. The Main Mongolian Lineament is marked by the dark black line – dashed red and black where it overlaps with a fault. Note the two conjugate strike-slip faults, the stacked thrusts at the basin margin and the two small transtensional basins located at the eastern and northern corners of the wedge. Cross sections C-C' and D-D' through the transtensional basin and the intersection wedge are shown. Cross-sections X2-X2' and X3-X3' are shown in Appendix A. . . . .	26
12	A cross-section through the Little Dariv Mountain area paired with a Landsat image of the surrounding area. Important locations and lithology are noted on the satellite image. . . . .	27
13	A cross-section through the Shargyn Fault in the northeast corner of the Shargyn Basin paired with a Landsat image of the surrounding area. Important locations and lithology are noted on the satellite image. . . . .	29
14	Offset stream beds along the ENE-WSW striking Shargyn Fault observed in Landsat imagery west of cross-section F-F'. . . . .	30
15	Shaded relief map of the Shargyn Basin showing blue plus signs where earthquakes have occurred between 1960 and 2013. Black lines are fault locations, like in Figure 7. Note that many of the earthquakes occur on, or near, mapped faults. However, three of the earthquakes occurred within the basin. . . . .	31
16	Schematic fault map of the Shargyn Basin region. The extent is approximately the same as the extent in Figure 3. Description of the structure is in the text. The shaded areas are basins. Unshaded areas are mountainous. The dotted lines represent the dominant foliation strike. The inset in the upper right is an even simpler description of the interacting stepover and wedge uplift. . . . .	32
17	Cross section X1 across the Butara Thrust on the southern margin of the Shargyn Basin, cross section X2 across the final terminal thrust of the Bogd Fault, and cross section X3 examining the Tonhil Fault and northwestern corner of the intersection wedge. . . . .	35
18	Cross section X4 through the Shargyn Fault at the southern margin of the Dariv Range and cross section X5 at the eastern margin of the Shargyn Basin. . . . .	36

# 1 Motivation

Continental deformation can occur far from plate boundaries. The behavior of intraplate fault systems is poorly understood. Furthermore, where multiple fault systems intersect, complex kinematics can occur. Understanding how and why these kinematic patterns develop is important for understanding broad active tectonic patterns, reconstructing past tectonics, analyzing seismic hazard and identifying potential resources.

In this paper, I examine the intersection of the Altai Range and the Gobi-Altai Range. The Altai Range and the Gobi-Altai Range are two large, actively forming mountain ranges in central Asia. The Altai Range is characterized by right-lateral transpressional slip, while the Gobi-Altai Range is characterized by left-lateral transpressional slip [Cunningham, 2005][Cunningham, 2010]. The intersection of these two fault systems provides a natural laboratory for studying strike-slip kinematics in an area with a long, varied tectonic history. Furthermore, an understanding of this critical zone will help elucidate the evolution of regional tectonic patterns.

The 150 km wide Shargyn Basin in western Mongolia lies at the intersection of the Altai fault system and the Gobi-Altai fault system. Here, I describe the Shargyn Basin as the result of transpressional strike-slip kinematics. The kinematics consist of a compressional strike-slip stepover, a conjugate strike-slip intersection, and termination thrust splays. I also discuss the active faulting in the context of pre-existing foliation and structural weaknesses.

## 2 Background on Mongolian Active Deformation

Understanding the tectonic context of the Shargyn Basin in western Mongolia and Asia is critical to interpreting the active deformation.

### 2.1 Mongolian Deformation in Context – Asia

Most of the active deformation in Mongolia is probably a result of the Indo-Eurasian collision [Yin, 2010][Walker et al., 2007][Cunningham, 2005][England and Molnar, 1997]. Indo-Eurasian collisional deformation processes can be separated into "kinematic" and "dynamic" models. The basic "kinematic" model suggests that the Indo-Eurasian collision has caused eastwards extrusion of crustal blocks towards the "free" eastern boundary (the East Asian Subduction Zone)[Tapponnier et al., 1982][Peltzer and Saucier, 1996]. This hypothesis suggests that most motion has been accommodated by large strike-slip and thrust faults. The "dynamic" models propose that the viscosity of the lithosphere is more important than upper crustal faults [Houseman and England, 1993][England and Molnar, 1997]. In these models, the important effects are continuous viscous deformation of the lithosphere and the gravitational effects of the resulting thickening.

Rollback on the East Asian Subduction System (EASS) provides an additional explanation for active and past motions in Mongolia [Schellart and Lister, 2005]. The EASS has been treated as a free-boundary in many of the East Asian tectonic models[Tapponnier et al., 1982][Peltzer and Saucier, 1996][Houseman and England, 1993]. But, because of its orientation, active EASS rollback would exert similarly oriented stresses to the Indo-Eurasian collision. However, the potential for far-field stresses from subduction zone rollback is not well constrained. Back-arc extension may not be limited to the deep, ocean-floor producing, back-arc basins. Much of the EASS was experiencing rollback during the late Cretaceous until the Mid-Miocene [Northrup et al., 1995][Schellart, 2005]. A physical model by Schellart and Lister [2005] showed that, if the entire East Asian Subduction zone were to rollback, intraplate deformation could occur as far as 3000 km from the subduction zone. Additional constraints on the active and past deformation in western Mongolia could influence these broad theories of Asian deformation.

The intensity of intracontinental deformation in Mongolia is emphasized by measured GPS motions and three of the largest strike-slip earthquakes ever. For a region so far from a plate margin, the rate of crustal deformation in Mongolia is very high. GPS measurements (Figure 2) show that ongoing motion is toward the north in the Altai, and mostly eastward in the Gobi-

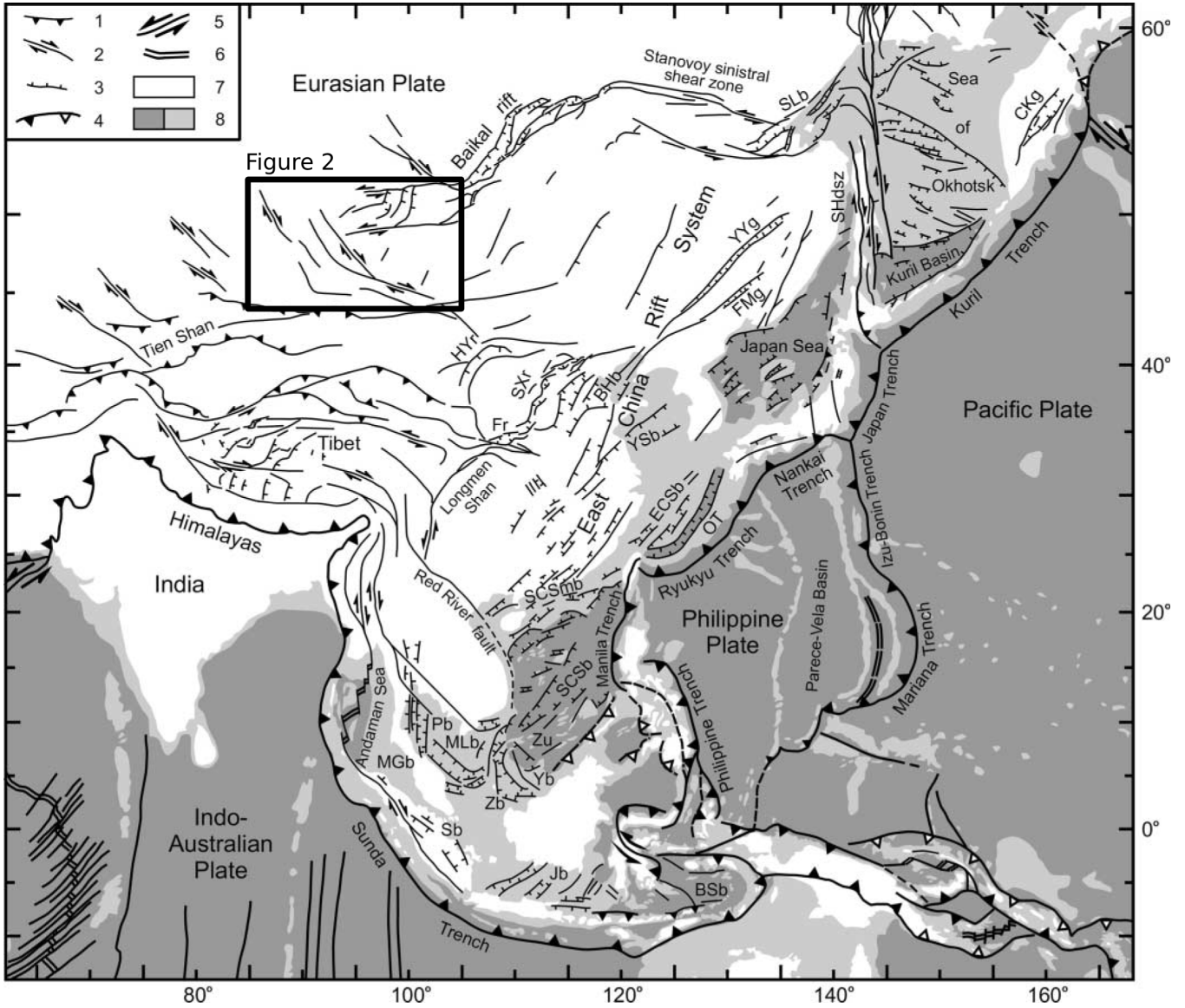


Figure 1: "Simplified tectonic map of East Asia and the Western Pacific illustrating latest Cretaceous and Cenozoic faults in East Asia. 1, 2 and 3 are major thrust, strike-slip and normal fault, respectively; 4, 5 and 6 are convergent (filled triangles are for active and open triangles are for inactive boundary), transform and divergent plate boundary, respectively; 7 is land; 8 is sea, with dark grey being basin or ocean floor and light grey being continental shelf or morphological high on basin or ocean floor. BHb, Bohaiwan basin; BSb, Banda Sea basin; CKg, Central Kamchatka graben; ECSb, East China Sea basin; FMg, Fushun-Meikehou graben; Fr, Fenwei rift; HYr, Hetao-Yinchuan rift; Jb, Java basins; MGb, Mergui basin; MLb, Malay basin; OT, Okinawa Trough; Pb, Pattani basin; Sb, Sumatra basins; SCSb, South China Sea basin; SCSmb, South China Sea marginal basin; SHdsz, Sakhalin-Hokkaido dextral shear zone; SLb, Shantar-Liziansky basin; SXr, Shanxi rift; Yb, Yunqing basin; YSb, Yellow Sea basin; YYg, Yilan-Yitong graben; Zb, Zengmu basin; Zu, Zenghe uplift" [Schellart and Lister, 2005]. The location of Figure 2 is outlined in Central Asia.

Altai[Calais, 2003]. The average rate of motion is approximately 5 mm/year relative to a stable Eurasia as defined by Calais [2003]. Multiple earthquakes with a moment magnitude of 8 or greater

have occurred in the last century. In July 1905, earthquakes with magnitude 7.9 and 8.4 occurred on the Bolnay Fault in northern Mongolia. The 1957, magnitude 8.0 earthquake on the Bogd Fault is one of the best exposed strike-slip surface ruptures in the world [Kurushin et al., 1998] [Okal, 1976] [Pollitz, 2003]. The Bogd Earthquake has been used as an analogue for potential Southern California earthquake events [Bayarsayhan et al., 1996]. The intensity of deformation makes Mongolia an ideal place to study the mechanics of intracontinental fault systems.

On the broadest scale, the Altai and Gobi-Altai fault systems may be related to a sequence of regularly-spaced, NW-SE striking right-lateral strike-slip faults [Yin, 2010] located in a belt from west Mongolia through Iran. The area is marked in the northwestern corner of Figure 1. Many of these faults terminate in large thrust systems like the Tian Shan. One explanation invokes bookshelf-like rotation along a long left-lateral shear zone creates the right-lateral faulting. [Davy and Cobbold, 1988][Bayasgalan et al., 2005] This model implies that the development of the Altai and Gobi-Altai is intimately linked to that of the Tian Shan. Possibly, the Altai and Gobi-Altai are similar to an earlier phase in the evolution of the Tian Shan, given the progressive northward propagation of stresses as the India-Eurasian collision proceeds.

Recent studies have examined the neotectonics of the Altai range via satellite imagery and targeted field excursions [Cunningham, 2005]. The region is dominated by NW-SE striking right-lateral slip. The primary features are strike-slip faults, but much of the topography is created by thrusts oriented 30 degrees off the main strike slip faults. Others are linked by a right-slip faults. In some places, the thrusts are part of a restraining bend. Major faults, GPS motions, and earthquake moment tensors are shown in Figure 2. Pure strike-slip, oblique slip and thrust earthquake moment tensors are observed, which indicates that active motion is variable depending on the specific fault [Bayasgalan et al., 2005]. The geologic slip rate for a major transpressional fault, the Hoh-Serh-Tsagaan-Salaa Fault, is 0.3 mm/yr of shortening and 0.9 mm/yr of dextral slip. This constitutes 20% of the total strain accumulation in the Altai. [Frankel et al., 2010]

Southeast of the Altai, deformation in the Gobi-Altai range is predominantly E-W striking left-lateral slip [Cunningham, 2010]. North and south dipping thrusts striking NW-SE follow the basement structures, whereas the strike-slip faults cut across the basement structures. The deformation is diffuse over a 250-350 km north-south extent. The range accommodates the eastwards and northeastwards deformation as measured by GPS. At the southern extent of the range, the Gobi-Tian Shan Fault is continuous from the easternmost Tian Shan through the eastern Gobi-Altai, thus supporting the connection between the Gobi-Altai and the Tian Shan. Some estimates sug-

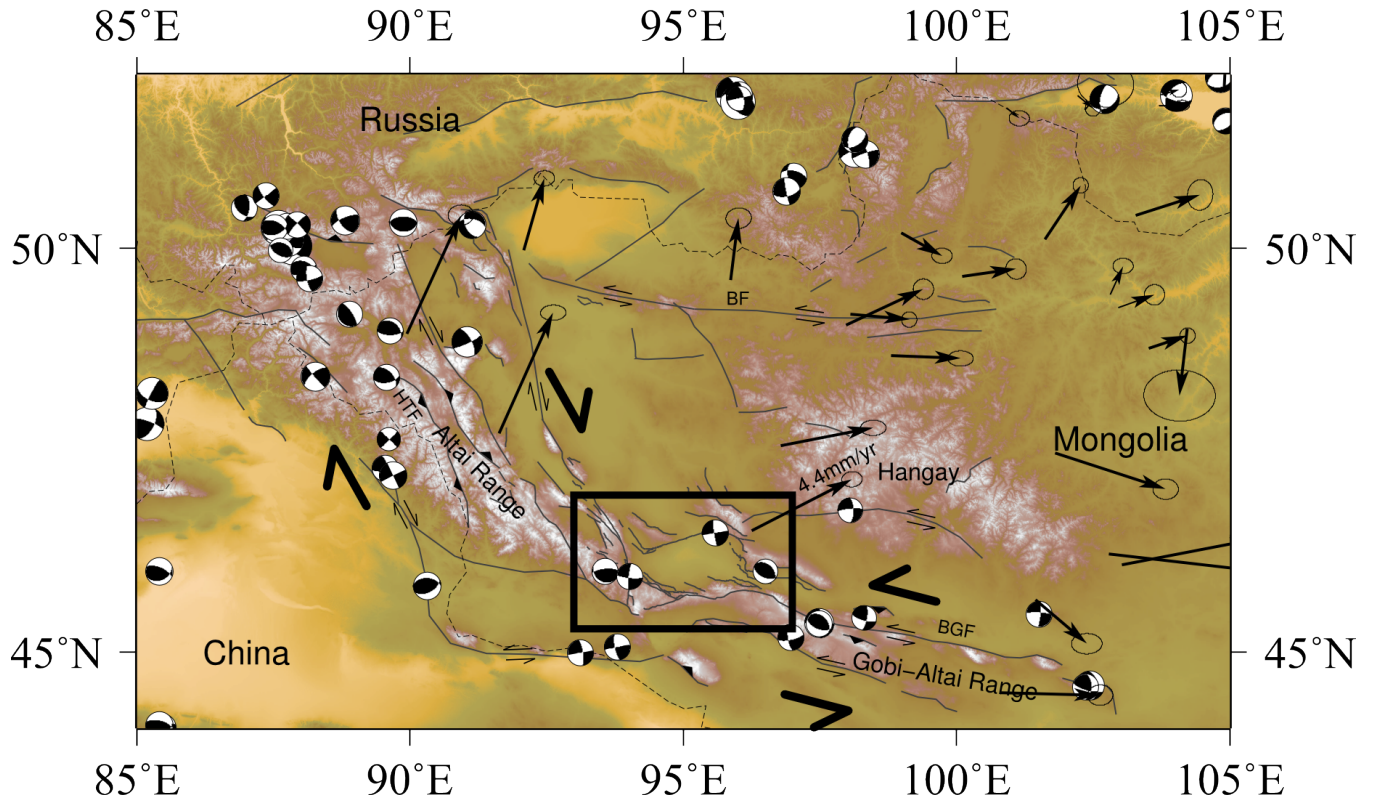


Figure 2: Shaded relief map of Mongolia with fault overlays and seismic moment tensor solutions for recorded earthquakes. Important locations or faults are labeled. HTF = Hoh-Serh-Tsagaan-Salaa Fault, BF = Bolnay Fault, BGF = Bogd Fault. The study area and location of Figure 3 is outlined in black. The difference between right-lateral transpressional strike-slip in the Altai Range and left-lateral transpressional strike-slip in the Gobi-Altai is especially important. Modified after Calais [2003]

gest 30-40 km of Cenozoic slip on the Gobi-Tien Shan Fault System (shown as "GBTS" in Figure 1) [Cunningham and Owen, 2003]. There are no slip estimates for the Bogd Fault System in the north. However, empirical relationships between fault slip and fault length suggest that the Bogd Fault System has experienced at least 10 km of slip [Cowie and Scholz, 1992]. Earthquake moment tensors show mainly left-lateral strike-slip in the Gobi-Altai.

Previous researchers have suggested that the Hangay Dome in central Mongolia (Figure 2) is a rigid block causing the formation of a pair of conjugate strike-slip faults (Altai and Gobi-Altai fault systems) [Cunningham, 2005]. However, recent detailed mapping work has shown the presence of large strike-slip structures cutting across the Hangay Dome [Walker et al., 2007]. This indicates that the Hangay Dome is being brittlely deformed in a similar fashion to the Gobi-Altai to the south, and may not be as rigid as previously thought [Walker et al., 2006] [Walker et al., 2007] [Walker et al., 2008].

## 2.2 Shargyn Basin

The Shargyn basin is located at the intersection of the Altai fault system and the Gobi-Altai fault system. It is approximately 150 km in east-west extent and 100km in north-south extent. A small ephemeral lake is located in the center of the basin. The basin margin varies between 1500 meters and 2000 meters, while the center is at an elevation of 963 meters. The basin is bounded on the west by the right-lateral Tonhil Fault and on the north by the left-lateral Shargyn Fault [Cunningham et al., 2003]. To the east and south, the tectonic regime is less certain. The Khantaishir Range to east has been the subject of petrological studies concerning the ophiolite located there. However, the mapping from these studies has not seriously examined the potentially active faults bounding the range to the southwest and west towards the Shargyn Basin. The neotectonics of the Bogd Range, which bounds the Shargyn basin to the south, are also poorly understood.

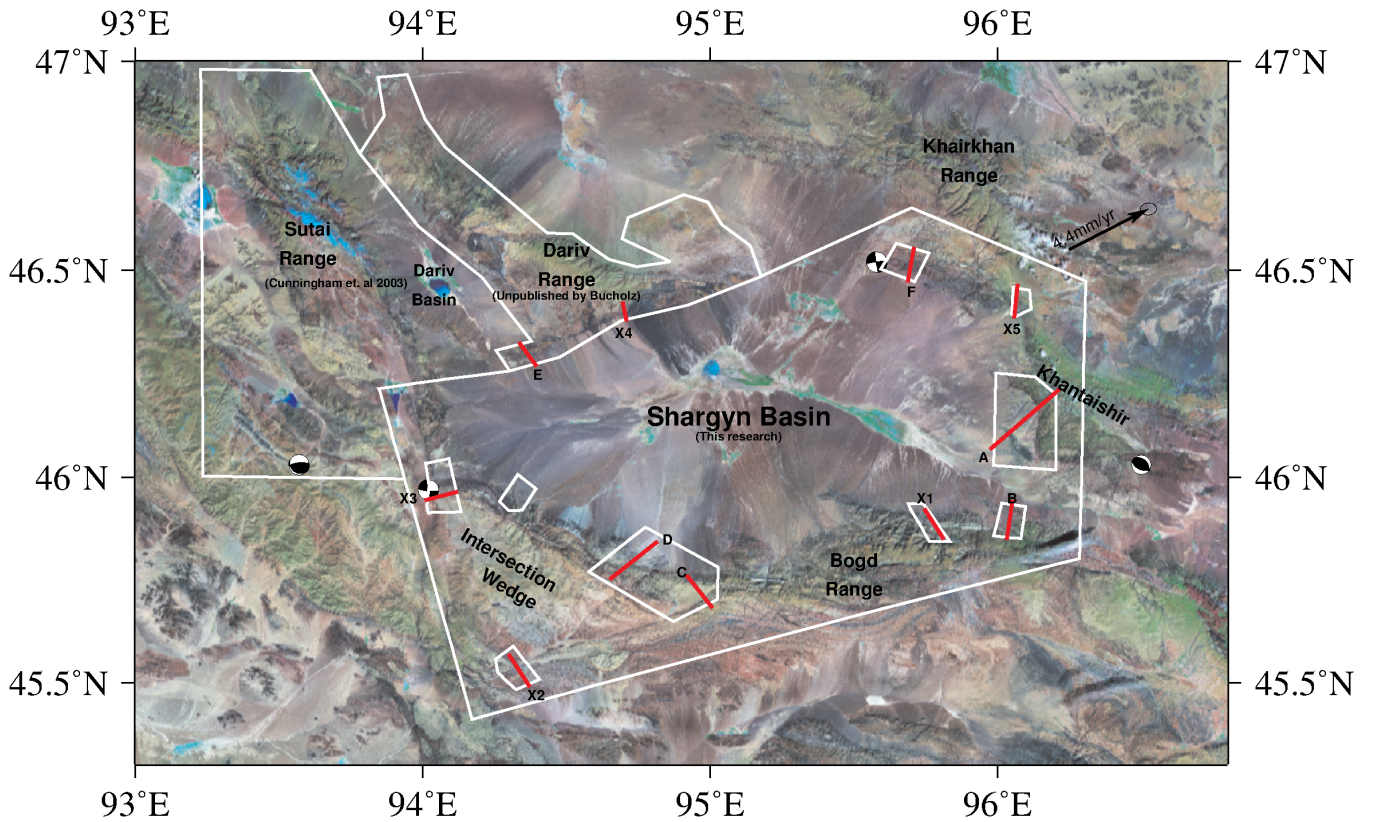


Figure 3: Landsat Imagery basemap showing important locations for this study. The large white box surrounding the Shargyn Basin is the new mapping from this study. The white area surrounding the Dariv Range indicates mapping performed by Dijkstra and Brouwer [2006] and as a part of unpublished research by Claire Bucholz. The area surrounding the Sutai Range was mapped by Cunningham et al. [2003]. The small white boxes around the Shargyn Basin show areas that we studied in the field. The red lines are labeled cross-sections that will be discussed in the Structural Evidence section. A GPS vector near the city of Altai is shown in the northeast. Earthquake focal mechanisms in the area are also shown.

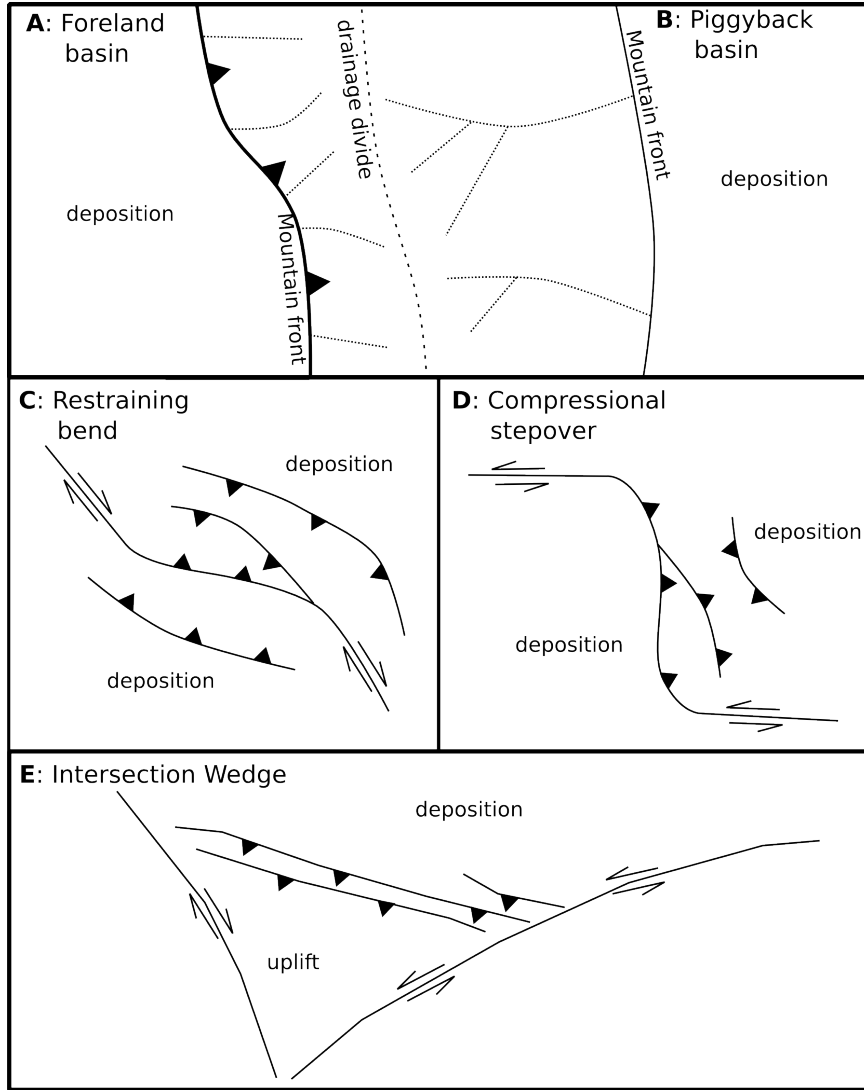


Figure 4: Schematic diagrams showing faulting and deposition for common transpressional uplifts and basins.

Many different types of basins form in strike-slip and compressional settings. Multiple types of basins can form and interact at the intersection of fault systems [Busby and Ingersoll, 1995]. Some of the settings we might expect:

- Foreland basins form in front of a simple thrust system. Flexural subsidence can result from the neighboring uplift. This is shown in Figure 4A.
- Piggyback basins form in the hinterland of a thrust fault. The adjacent uplift provides a sediment source. Shown in Figure 4B
- Restraining bend basins form similarly to foreland basins with deposition in the foreland of thrusts, but often form on both sides of a positive flower thrust structure. Shown in Figure

- Compressional stepover basins form similarly to restraining bend basins. However, rather than a bend in the primary strike-slip system, there are two parallel strike-slip fault segments, separated by at least one thrust fault. In the compressional case, the basin is essentially a foreland basin in front of the thrust. Arguably, these fault systems are just large restraining bends. Shown in Figure 4D.
- An intersection wedge can form at a conjugate strike-slip intersection. Because strike-slip motion on both faults must be transferred into uplift, an uplifted wedge of material forms between the two faults. Shown in Figure 4E

A goal of this paper is to describe the Shargyn Basin in these terms. A summary of the results is in the Structural Interpretation section. Nearby regions have already been investigated. Not quite bordering the Shargyn Basin, to the northwest, is the Sutai Range. The Sutai Range is the largest mountain range in the region, with an ice-capped summit above 4000m. It represents the southeastern-most uplift in the Altai. The Sutai Range is an active restraining bend in the Altai fault system[Cunningham et al., 2003][Howard and Cunningham, 2006]. A stepover in the right lateral fault has resulted in progressively more thrusting. The faults bounding the range exhibit a positive flower structure such that the faults on the east dip to the west and the faults on the west dip to the east[Cunningham et al., 2003].

To the east of the Sutai Range, the Dariv Thrust uplifts the Dariv Mountains. Howard and Cunningham [2006] describe the Dariv Basin as a piggyback basin, riding on top of the block thrust up by the Dariv Thrust. The Dariv Basin could also be described as a restraining bend basin from deposition and subsidence due to the adjacent Sutai Range. On the northern boundary of the Shargyn Basin, the Shargyn fault, a left-lateral strike slip fault, bounds the southern edge of the Dariv Mountains, separating the Shargyn Basin from the Dariv Basin.

## 2.3 Bedrock Geology

The bedrock in western Mongolia formed as part of the Central Asian Orogenic Belt. The Central Asian Orogenic Belt formed from 1000 Ma to 250 Ma as an agglomeration of island arcs, accretionary wedges, ophiolites and microcontinents in a complex multiphase development similar to what is

seen today in southeast Asia [Windley et al., 2007]. The broad tectonostratigraphic provinces in Mongolia are shown in Figure 5.

The Shargyn Basin lies near the Main Mongolian Lineament (MML), a boundary between rocks of very different ages. North of the MML, Proterozoic and early Paleozoic units are present, whereas on the southern side of the MML, there are Silurian and Devonian gneiss, schist and felsic igneous rocks. The area is dominated by greenschist facies accretionary complex units. In the Dariv Range, arc-related igneous units are prevalent. The northern end of the Dariv Range and the bulk of the Khantaishir Range consist of ophiolite-related mafic and ultramafic units. To the south of the Main Mongolian Lineament, the units are primarily Silurian and Carboniferous arc-related metamorphic and igneous rocks. Another phase of regional magmatism may have occurred during the Permian [Windley et al., 2007]. Small, post-orogenic sedimentary basins are also present throughout the region.

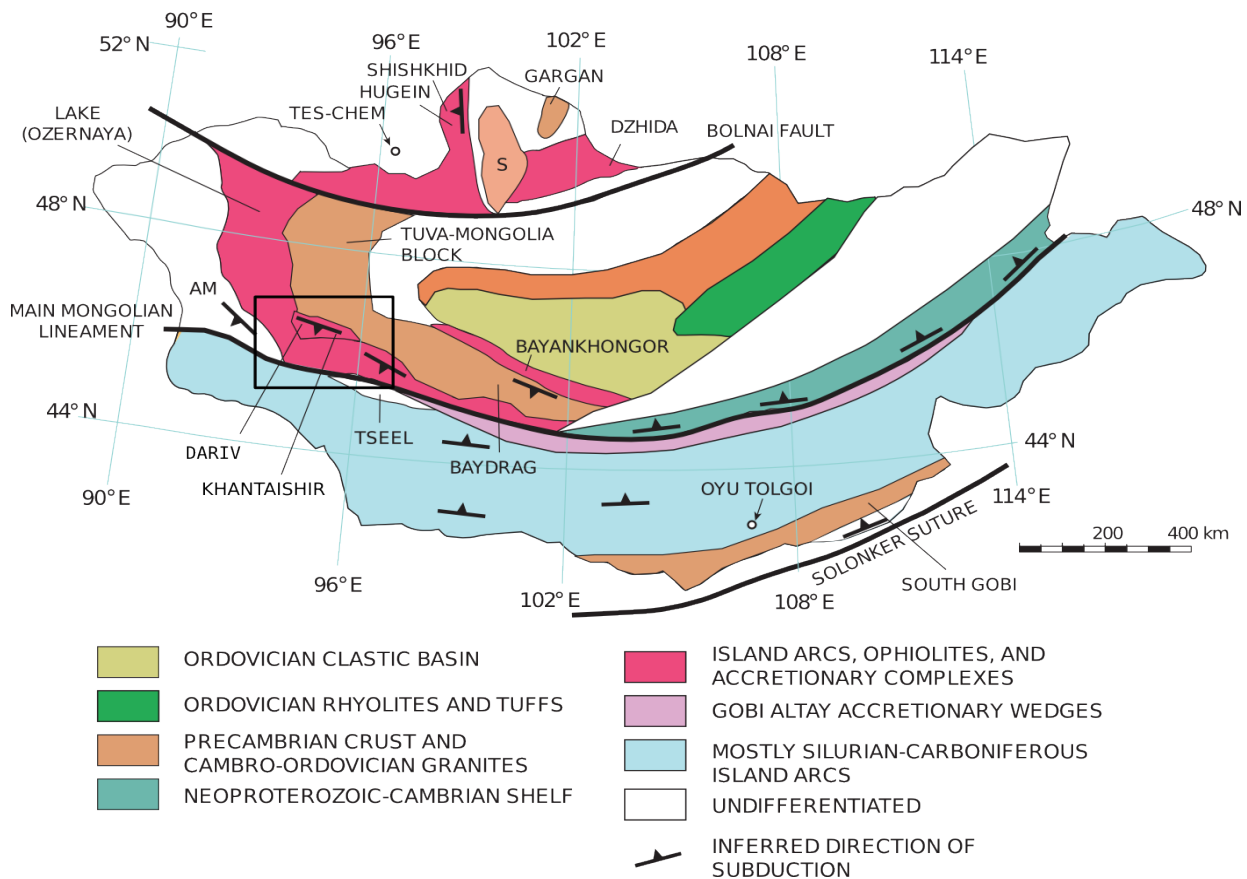


Figure 5: Schematic tectonostratigraphic map of Mongolia. The area we studied is located in the outlined box. The Main Mongolian Lineament is the black line passing through our study region. Credit to Windley et al. [2007]

The structural grain of these Paleozoic orogenies could affect the location of present day faults,

because the metamorphic foliation represents a major plane of weakness. The dominant structural grain of the Central Asian Orogeny is shown in Figure 6. There is a close correspondence between the major faults and this structural fabric.

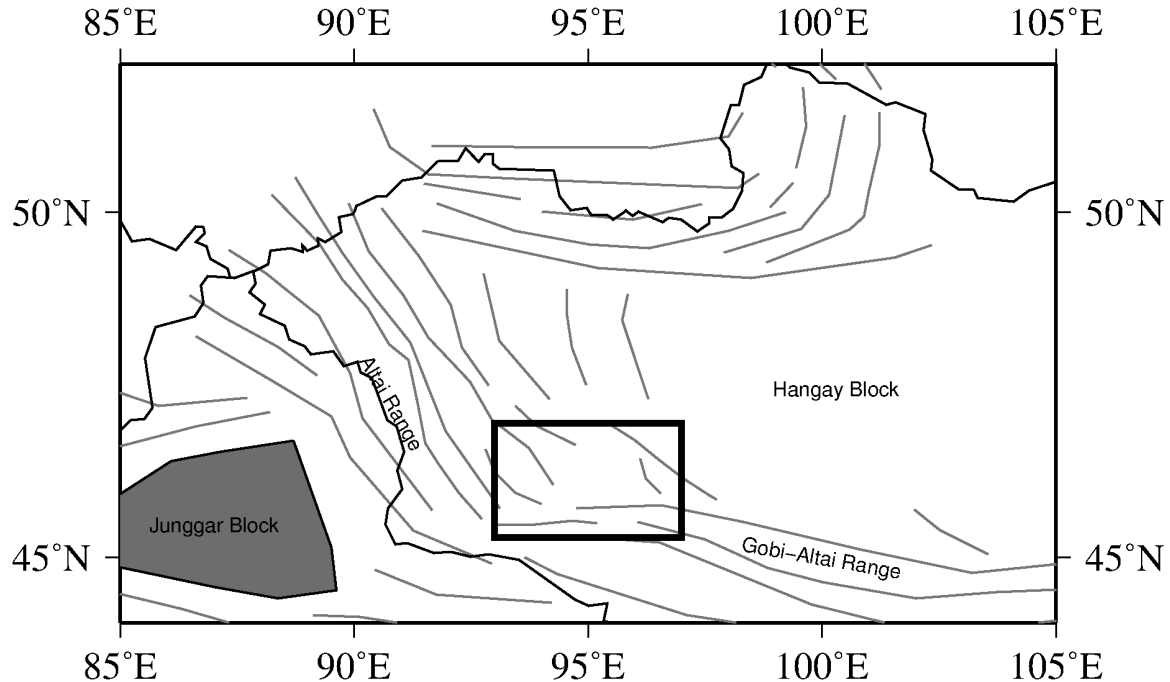


Figure 6: Schematic map of the dominant structural grain in western Mongolia. The study area is boxed for reference. The shaded Junggar Block is mechanically rigid. The Junggar Block may be a trapped block of oceanic crust [Carroll et al., 1990]. The Hangay Block consists of microcontinental fragments that accreted during the early stages of the Central Asian Orogeny. It is not shaded because it is probably not mechanically rigid. Modified after Cunningham [2005]

### **3 Structural Evidence**

#### **3.1 Remote Sensing**

Previous studies have examined Mongolian active tectonics from a remote sensing perspective [Cunningham, 2005][Cunningham, 2010][Tapponnier and Molnar, 1979][Walker et al., 2007]. I performed a more detailed remote sensing survey of the Shargyn Basin region using Landsat 7 TM+ satellite imagery. Surface features indicating active motion were identified. Because the region is arid, many important features are clearly visible. For example, the trace of Tonhil Fault on the western margin of the Shargyn Basin is visible as a very sharp linear topographic feature. Using such features from Landsat imagery was useful in identifying important features for further investigation in the field. Using contiguous features on the satellite imagery, field mapping results can be extended to nearby, unobserved areas.

In the remote sensing studies, I focused on identifying prominent faults using steep topography, sharp color changes (lithology changes), fault scarps, and offset features. I also mapped clearly distinguishable lithologic units using color, weathering, and foliation changes visible in the Landsat imagery. Where possible, I noted the strike of the foliation. Foliation is useful to map out the Paleozoic structural grain in the region. I also noted the location and distribution of alluvial fans. Locations where alluvial fans are forming above active thrusts are important because that might indicate a temporal or slip difference between multiple adjacent faults.

#### **3.2 Field Mapping**

During the summer of 2012, Claire Bucholz, myself, and Yeson Erdene, a student at Mongolian University of Science and Technology performed two months of fieldwork in the Shargyn Basin region. We spent part of the time focusing on the active faults. We performed 10-20 km transects through areas with important faults, as previously identified by satellite image (mostly similar to the faults identified by [Walker et al., 2007]). We mapped at a broad scale, but made careful note of features indicating recent brittle deformation. Topography, fracturing, fault exposures and shifts in foliations or lithology were all important in locating faults. Mapping was performed on paper with the assistance of satellite imagery and a GPS device. Later, the mapping was transferred to digital form.

The results of this mapping are summarized in a fault map in Figure 7. Published mapping

in the Sutai Range by Cunningham et al. [2003] and in the Dariv Range by Dijkstra and Brouwer [2006] is incorporated. Further unpublished mapping of the Dariv Range by Claire Bucholz is incorporated. We performed new mapping surrounding the Shargyn Basin. Eleven cross-sections were created. Six of these are shown in the text. The remaining cross-sections are in Appendix A. The following sections describe in detail the important structural results, while referencing these cross-sections.

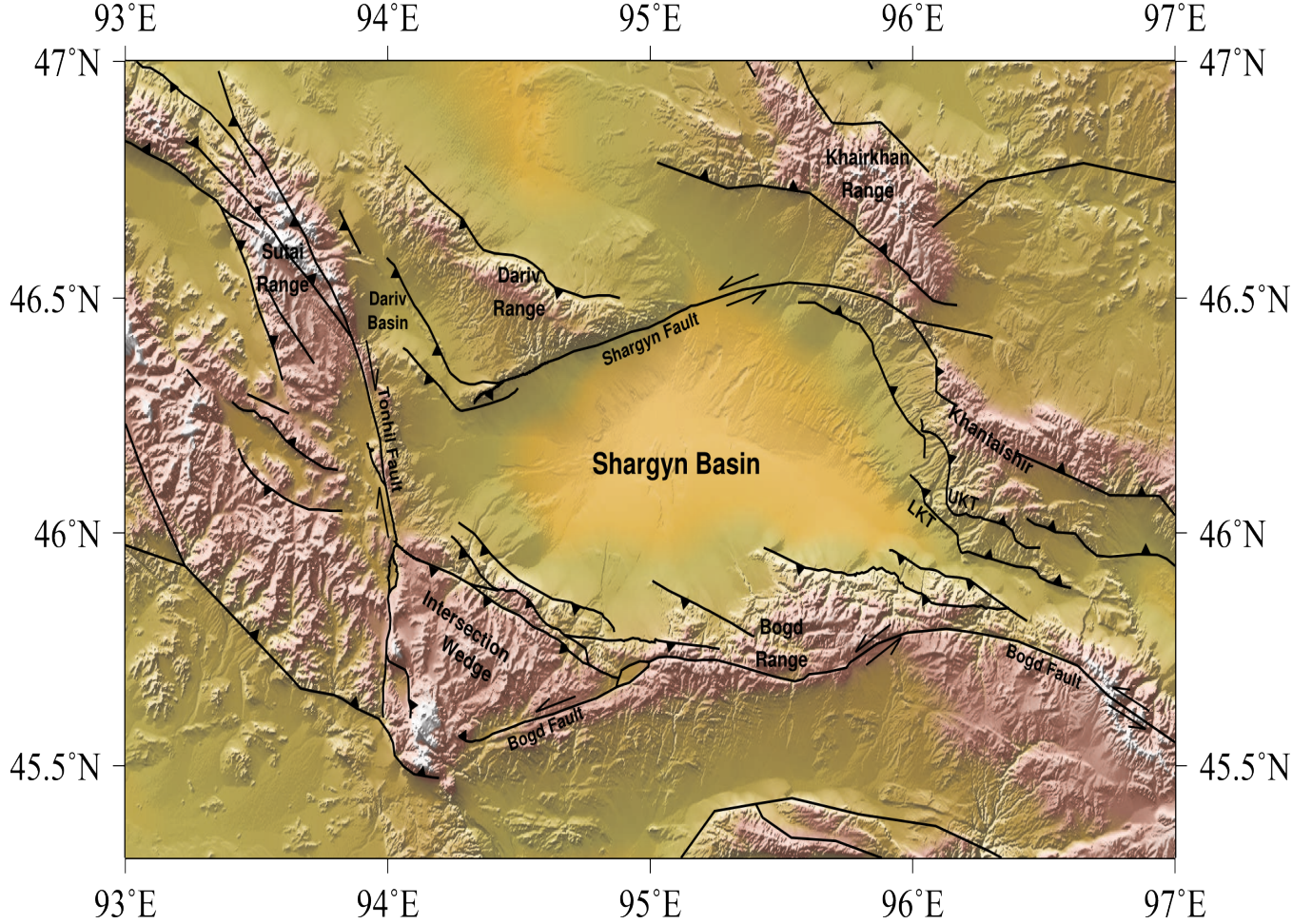


Figure 7: A map of the Shargyn Basin showing the studied faults and important locations. Slip is indicated by thrust teeth or lateral slip arrows.

### 3.3 Khantaishir Thrusts

The eastern edge of the basin is uplifted with motion concentrated on two faults which I call the Upper Khantaishir Thrust (UKT) and the Lower Khantaishir Thrust (LKT). The cross-section across these two faults is marked on the map as A-A'. Other minor faults are identifiable on the satellite imagery. We did not investigate the minor faults in the field. Both the UKT and LKT

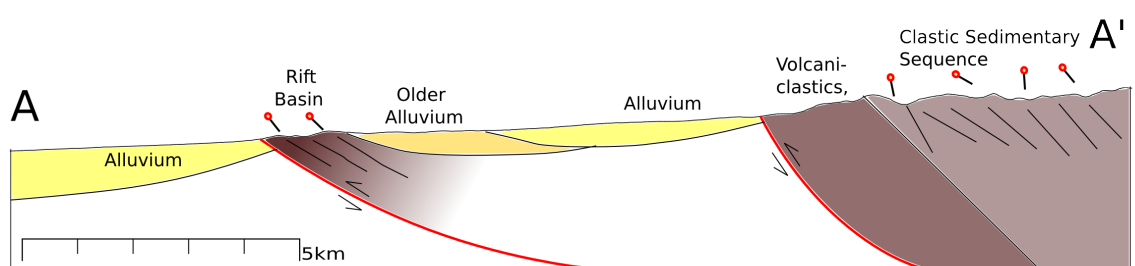
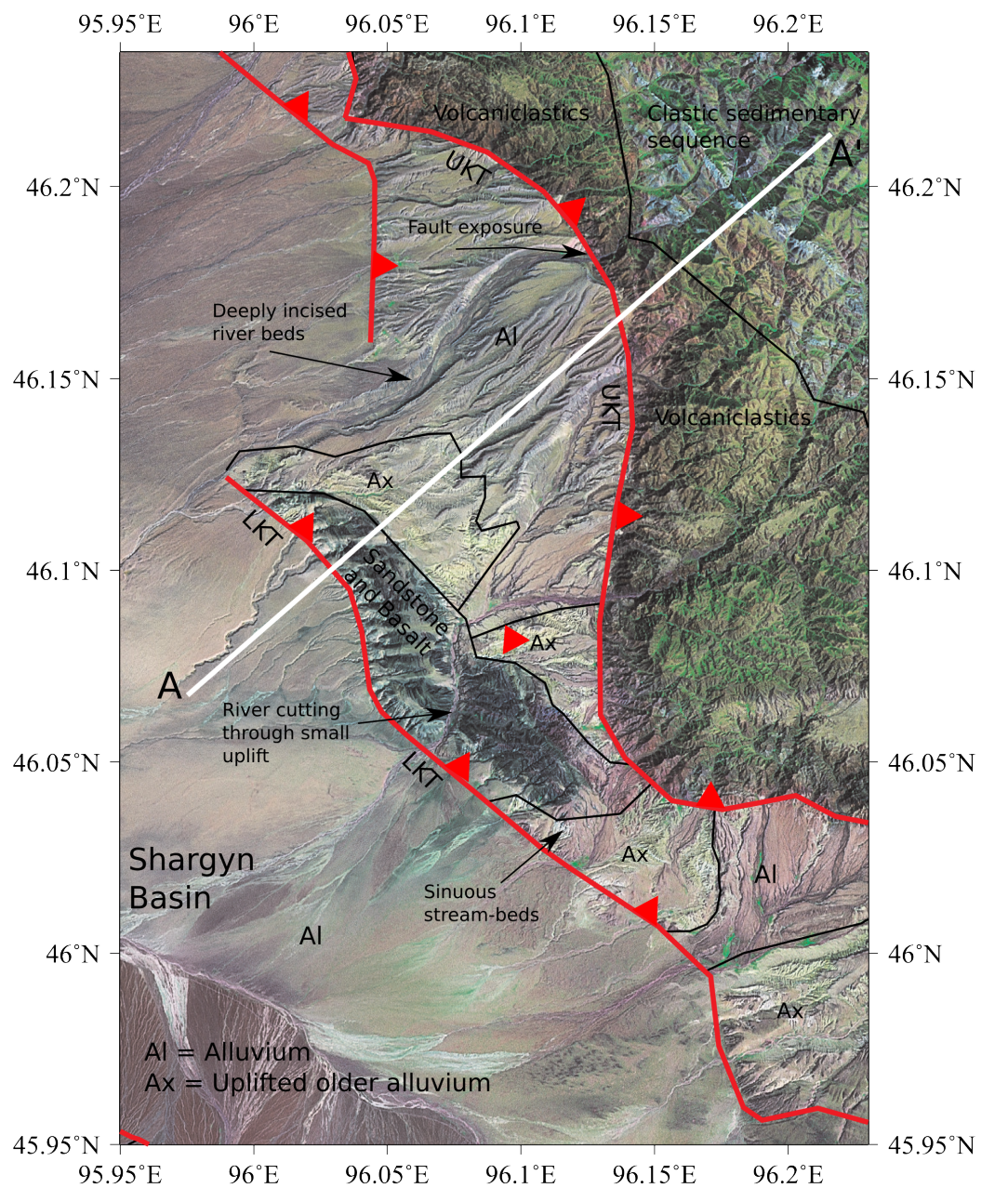


Figure 8: A northeast-southwest cross-section through the Khantaishir Range and the Khantaishir Thrusts paired with a Landsat image. Important locations and lithology are noted on the satellite image.

strike approximately NNW-SSE. The UKT is the northern fault. On the northeast side of the UKT, we observed a thick fractured layer of volcaniclastics underneath a sedimentary sequence with a thick conglomerate layer followed by shales, sandstones and carbonate reef deposits. At higher elevations in the mountain range, mafic and ultramafic ophiolite-related rocks are present. No outcrop is found on the southwest side of the UKT. At the alluvium-outcrop transition, we observed a 3-5m wide deformation zone that we interpret as the UKT itself. This zone is shown in Figure 9A. Nearing this thrust trace, there is a significant increase in fracturing with strikes between  $280^{\circ}$  and  $320^{\circ}$ . Fracture dip was similar to the dip of the UKT itself. Rotated sigmoidal tension gashes were observed immediately above the deformation zone indicating a thrust sense of motion. S-C fabric within the deformation zone also indicated thrust motion.

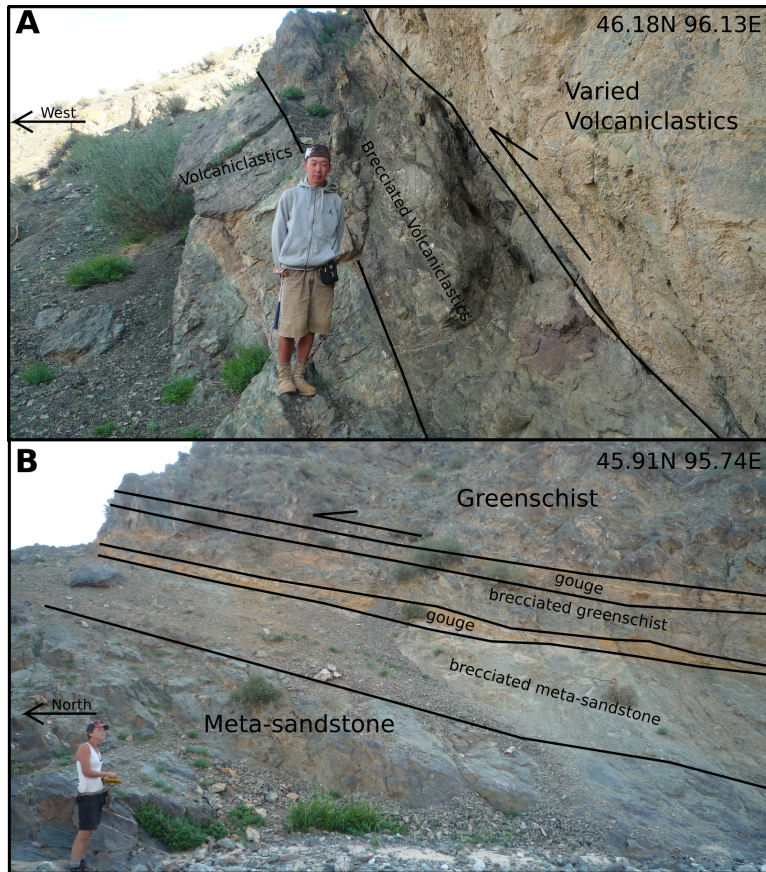


Figure 9: Photographs of exposed faults. Field workers are used as scale bars. A) An outcrop of the exposed Upper Khantaishir Thrust from cross-section A-A'. B) An outcrop of the exposed thrust in cross-section X1-X1'

The trace of the Lower Khantaishir Thrust (LKT) is located 10km to the southwest of the UKT. South from the UKT, there is a transition from recent alluvium to more lithified, potentially older alluvium. Then, for 2 kilometers before reaching the LKT, there is a thick stack of sandstone and

basalt flows, with interlayered sandy carbonate beds. Finally, there is a very sharp topographic transition and lithologic shift to recent alluvium. This marks the fault trace for the LKT. The sedimentary sequence northeast of the LKT indicates the presence of a minor basin in the area at a point after the widespread metamorphism affecting the area.

Motion on the LKT may have begun after the motion on the UKT. In the small uplifted region near the trace of the LKT, there are deeply incised, but highly sinuous incised drainage canyons. Such incised drainages indicate that, before uplift began, a pre-existing sinuous drainage pattern existed. The uplift was rapid enough that the drainage pattern was "locked in". Because these drainages are aligned with the current southwestwards drainage patterns from the Khantaishir Range and the UKT, it fits with a southwestwards drainage pattern for the time-period before the LKT was active. The deep drainages between the LKT and the UKT also indicate that the LKT is a later uplift. A major drainage cuts through the uplift adjacent to the LKT. Such a drainage would be unlikely to form unless it was present before the activation of the LKT, providing further evidence that uplift began on the UKT before beginning on the LKT.

### 3.4 Bogd Fault and Termination Thrust Splays

Along the southern margin of the basin, we performed two transects across two thrusts splayed off the Bogd left-lateral strike slip fault. We will refer to the northern thrust as the Haliun Thrust and the southern thrust as the Butara Thrust. Above (south) of the Haliun Thrust, there is a complex sequence of metasedimentary and metavolcanics rocks that are intruded by a large gabbro body. There might be a fault-adjacent anticline. I do not know whether such an anticline is actively forming or a remnant from previous orogenies. The foliation in the fault-adjacent units is parallel to the Haliun Thrust and dips to the south. Along the basin margin, elevations decrease to the west. The decrease in elevation indicates the uplift tapers off further from the Bogd strike-slip fault.

To the south of the Haliun Thrust, the Butara Thrust uplifts 3000m high peaks in the center of the Bogd Range. To the north of the Butara Thrust, we observed the same metasedimentary sequence as is adjacent to the Haliun Thrust. To the south of the Butara Thrust, there are sandstones and basaltic units. Just to the west of the cross-section, alluvium is accumulating south of the Haliun Thrust, indicating that more of the uplift is occurring on the Butara Thrust. To the west of cross-section, the high topography is almost entirely south of the Butara Thrust.

The Butara Thrust is exposed 25 km west of cross-section B-B'. Data from a transect performed

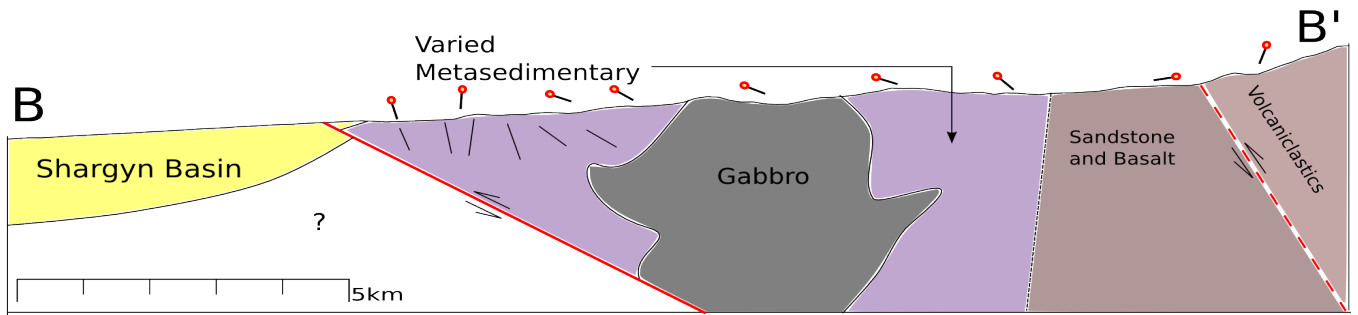
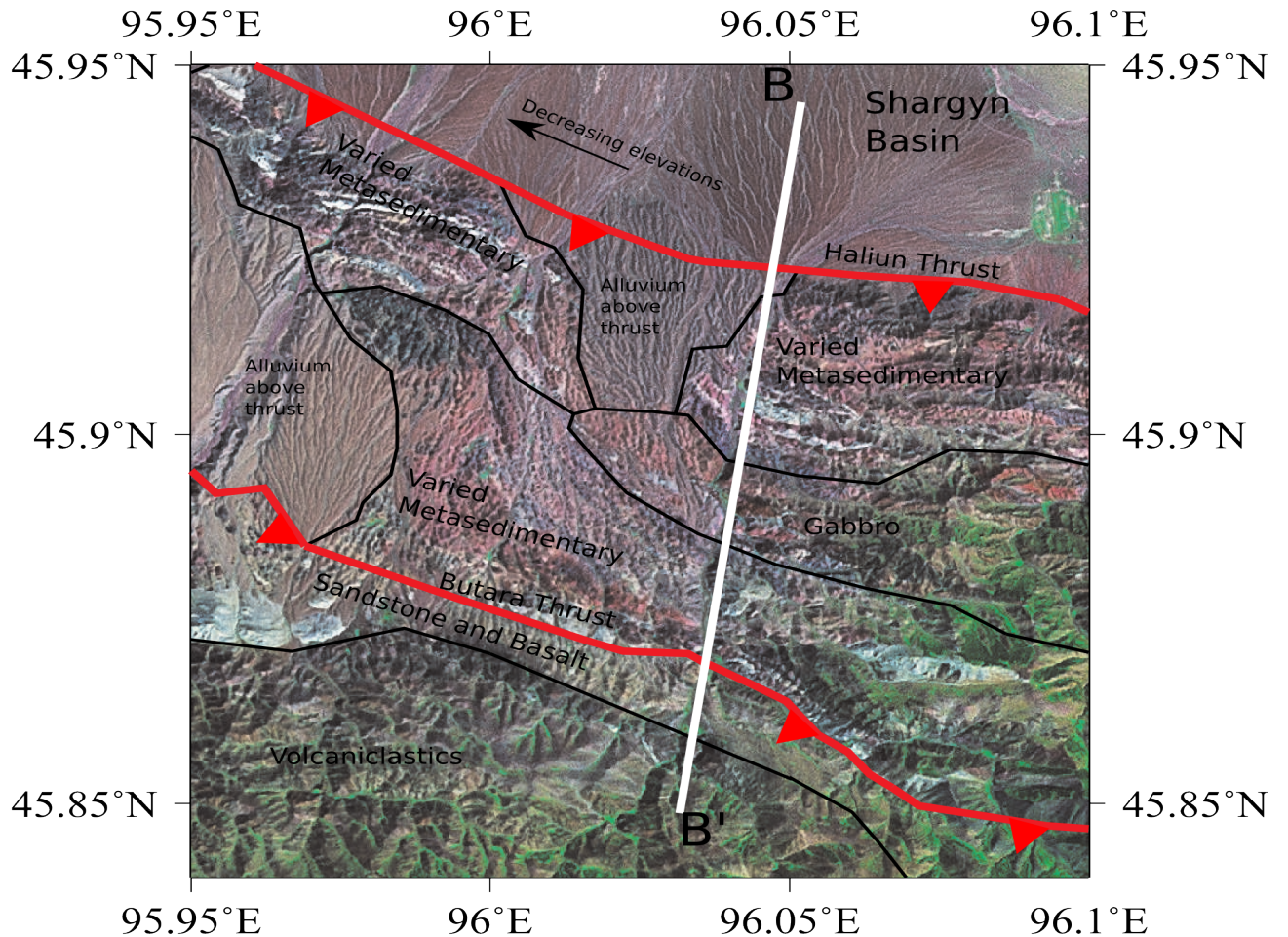


Figure 10: A cross-section through the Haliun Thrust and Butara Thrust paired with a Landsat image. Important locations and lithology are noted on the satellite image.

at this location is shown in cross-section X1-X1' in Appendix A. Based on the outcrop, the fault strikes E-W and dips 15°. The foot wall consists of low grade metamorphosed mudstones and sandstone. The hanging wall consists of greenschist. Inwards, there are multiple layers of brecciated footwall and hanging wall rock and multiple layers of fault gouge. Kinematic indicators suggest thrust sense of motion. A photograph is shown in Figure 9B. The topography rises sharply directly south of the location of the fault.

Further west, there is a third thrust splay off the Bogd Fault that can be seen in Figure 7. But, we did not visit this fault in the field map. The satellite imagery suggests that it is similar in nature to the Haliun Thrust and the Butara Thrust.

### 3.5 Tonhil Fault and Intersection Wedge Thrusts

On the south-western margin of the Shargyn Basin, the wedge between the Tonhil Fault and Bogd Fault exhibits some of the most extensive thrusting.

At the eastern corner of the intersection wedge, there is a bend in the Gobi-Altai Fault from E-W striking to ENE-WSW striking. At the location of this bend, there is a small (2 km wide) transtensional basin, shown in cross-section C-C'. This has been previously identified on satellite imagery by Cunningham [2010]. We examined the area in the field. Though we were not able to directly observe any deformation structures, the southern margin of this basin had a very steep topographic rise. North of the basin, we found a large granite intrusion. South of the basin, there are south dipping high grade metamorphic rocks. Because of the topographic depression and local deposition, the small basin is probably bounded by a normal fault on one side and the left-lateral Bogd Fault on the other.

At cross-section D-D' (shown in Figure 11, we performed a transect through the series of thrusts separating the basin from the intersection wedge. At the site of the transect, there are three thrusts. The lowest thrust marks the basin margin. To the southwest of this thrust, there is a large hornblende-rich diorite intrusion with minor intrusions of granite included. Close to the middle thrust, there is sedimentary sequence that includes an actively mined coal bed. The middle thrust causes a noticeable topographic jump. On the southwest side of the middle thrust, there are intrusions of gabbro and diorite. The southwesternmost thrust separates these intrusive rocks from a schist and carbonate unit. To the southwest, the topography levels out onto a broad plateau over the whole intersection wedge area. Based on the topography, each of these faults accommodates some portion of the intersection wedge uplift. However, digital elevation profiles separating the basin and the intersection wedge point to along-strike variation in how much uplift is accommodated on each of the faults.

The western boundary of the intersection wedge is controlled by the Tonhil Fault. The Tonhil Fault is a major NNW-SSE striking right-lateral strike slip fault. At the cross-section X3-X3' (shown in Appendix A), we examine the fault where it interacts with the northwestern corner of

the intersection wedge. At the latitude of the cross-section, the Tonhil fault bends so that it strikes nearly N-S. This bend appears to have created another transtensional basin. We did not examine the transtensional basin in the field. It is intriguing that it lies symmetrically across the intersection wedge from the transtensional basin on the Bogd Fault examined in cross-section C-C'.

Further east, along cross-section X3-X3', we observed a boundary between greenschist grade metasedimentary rocks on the east side and a gneissic unit on the west side. This is interpreted as the furthest northern extent of the southwestern-most of the intersection wedge thrusts. For most of its length, satellite imagery of this fault shows some topographic expression and where observed in the field, it always separates the gneiss and schist from the metasedimentary rocks, indicating that it is an important structural boundary.

At the far southern corner of the thrust wedge, we examined the terminus of the Bogd Fault, shown in cross-section X2-X2' in Appendix A. After the various thrust splays further east and north, it is unlikely that there is significant relative motion so far south. However, what remains is directed into a thrust fault that strikes approximately 45 degrees off the main Bogd Fault. There is a noticeable topographic rise bending away from the main Bogd Fault. The small depositional region and the topographic rise would be unlikely without recent motion. In addition, there was a high degree of fracturing.

### 3.6 Shargyn Fault and Termination Thrust Splays

The northern margin of the basin is separated from the Dariv Range by the Shargyn Fault. Four of the transects focus on this fault. The fault strikes WSW-ENE. In the cross-sections, I have assumed that the Shargyn Fault is approximately vertical because of its lateral slip and the lack of other constraints.

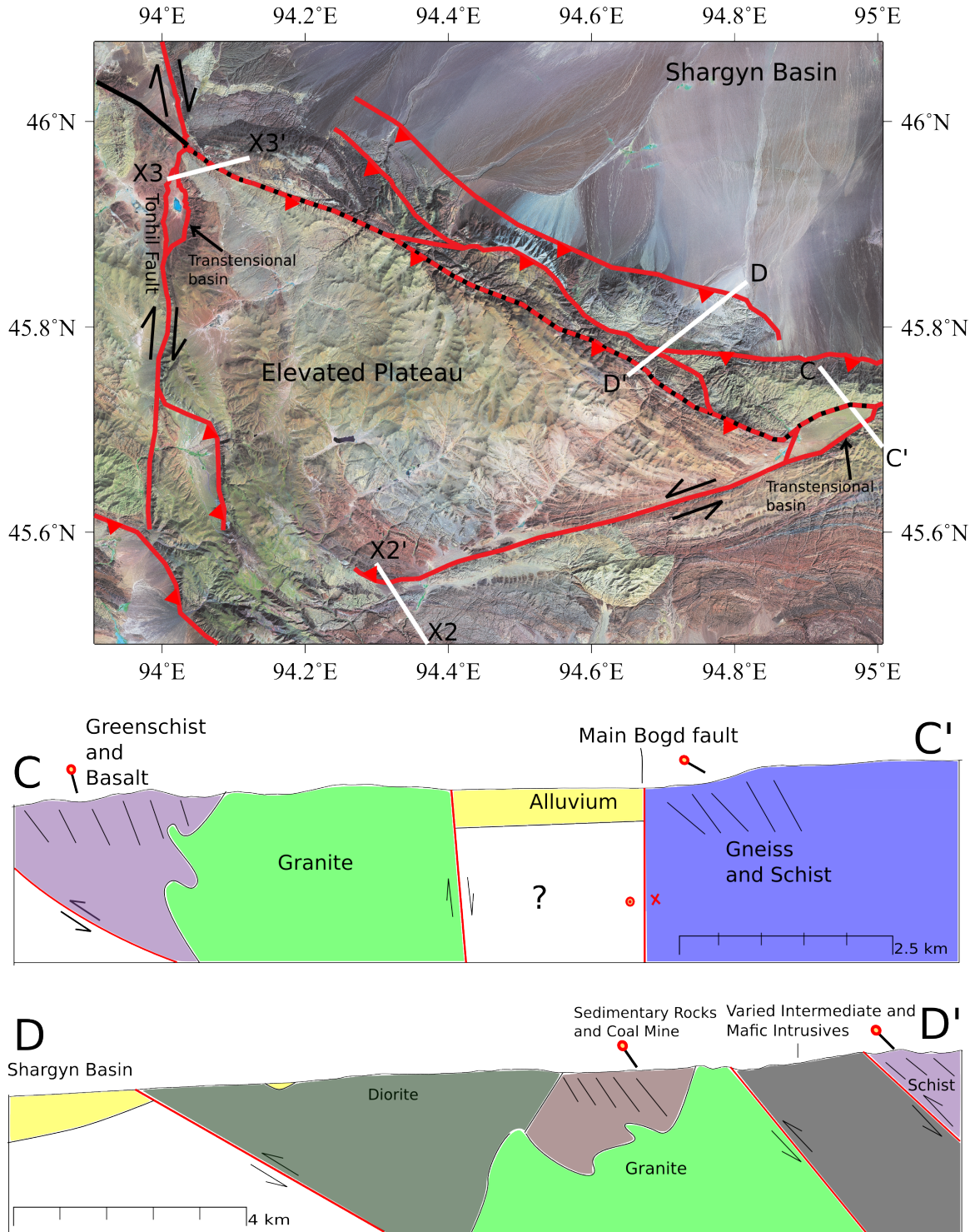


Figure 11: Landsat imagery showing the intersection wedge area at the southwestern corner of the Shargyn Basin. Mapped active faults are shown by solid red lines. Slip sense is shown with thrust teeth or lateral slip arrows. The Main Mongolian Lineament is marked by the dark black line – dashed red and black where it overlaps with a fault. Note the two conjugate strike-slip faults, the stacked thrusts at the basin margin and the two small transtensional basins located at the eastern and northern corners of the wedge. Cross sections C-C' and D-D' through the transtensional basin and the intersection wedge are shown. Cross-sections X2-X2' and X3-X3' are shown in Appendix A.

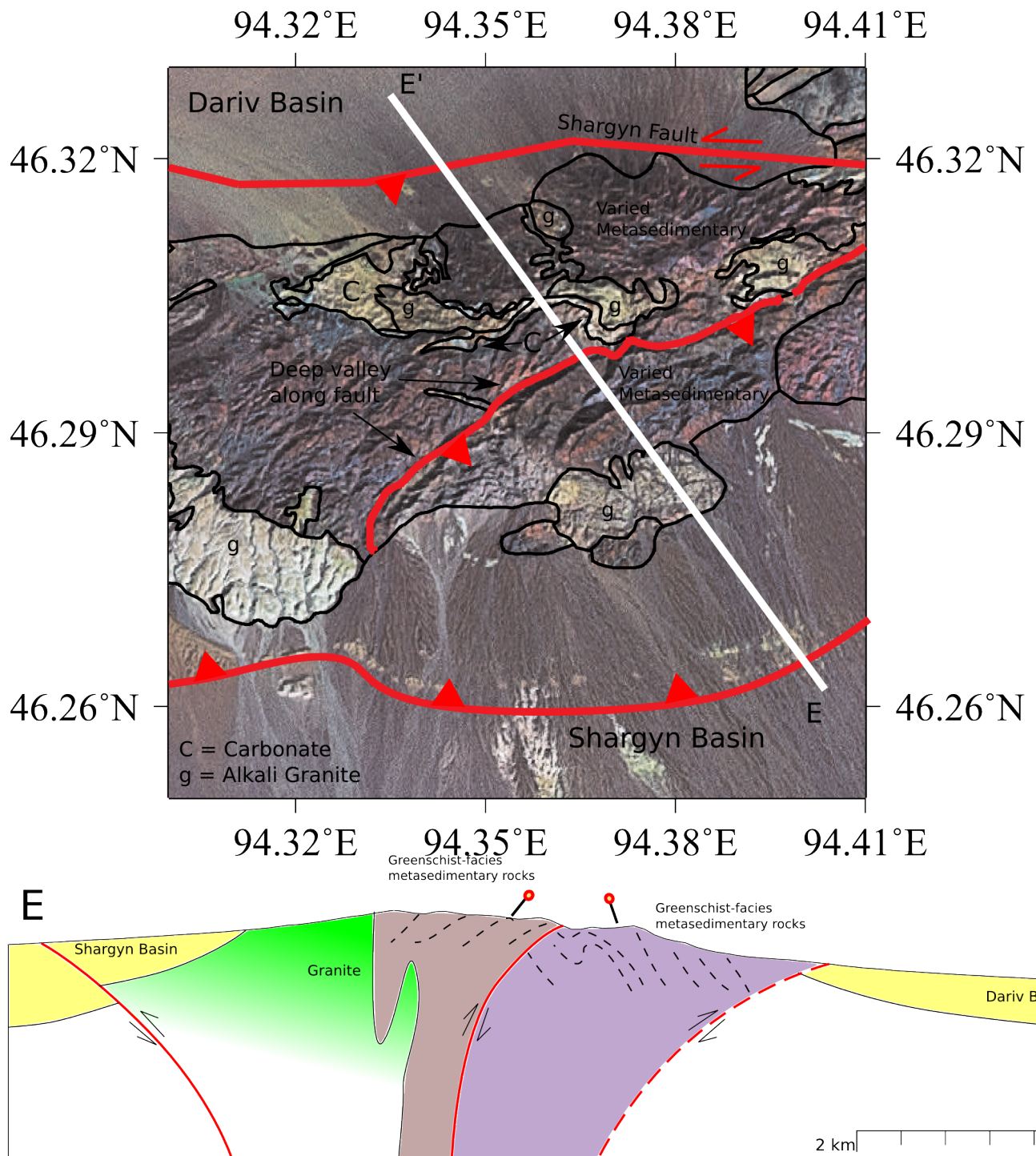


Figure 12: A cross-section through the Little Dariv Mountain area paired with a Landsat image of the surrounding area. Important locations and lithology are noted on the satellite image.

The western end of the Shargyn Fault, nicknamed Little Dariv Mountain, exhibits thrusts in a small positive flower structure, seen in cross-section E-E' in Figure 18. The positive flower structure has been identified by previous researchers [Howard and Cunningham, 2006]. Their interpretation is similar to the one discussed here. However, there are differences in the number and location of thrusts. To the north of the Shargyn Basin is the Dariv Basin, a much smaller, higher elevation basin. Little Dariv Mountain is located on the boundary of these two basins. The majority of the mountain is composed of greenschist-facies sedimentary and volcanic rocks. On the northern side of the range, there is a 100 meter thick band of folded carbonates and marls. Separating the range is a thrust fault. The fault follows a valley that is clearly visible on satellite imagery. To the south of the fault is a steep 200 meter topographic rise, indicating that the fault dips southwards. No other faults were identifiable in the core of Little Dariv Mountain.

On the cross-section, two other faults are indicated on the periphery of the mountain. The southern fault can be seen in the satellite imagery as an uplifted trace of bedrock amongst a sea of basin sediments. It may be related to a large anticline visible on the satellite imagery west of Little Dariv Mountain. The northern boundary fault is the inferred continuation of the main Shargyn Fault trace. This continuation of the Shargyn Fault terminates as thrust motion on thrusts in the Dariv Basin. Because the Dariv Basin thrusts are the easternmost extent of the Sutai Range restraining bend [Cunningham et al., 2003], the thrusting involved in the Sutai Range restraining bend can be linked with the strike-slip motion on the Shargyn Fault.

In the central south of the Dariv Range, we examined a simple section of the Shargyn Fault, marked X4-X4' in Figure 3 and shown in Appendix A. To the north, the topography rises steeply towards a relatively flat plateau. The bedrock is composed of serpentinite, biotite-gabbro and gabbro-diorite, separated by intrusive contacts. Despite the steep topographic rise at the fault, it is unlikely that there is any dip-slip on the Shargyn Fault here. Thrusting on the Shargyn Fault at this location would conflict with the lack of topographic expression along the fault east of the Dariv Range. It is more likely that the Dariv Thrust to the northeast is uplifting the range and the Shargyn Fault is simply accomodating the juxtaposition of the uplifted Dariv Range and the Shargyn Basin.

In the northeastern part of the basin, the Shargyn Fault and a small adjacent thrust are shown in cross-section F-F' (Figure 13). The small thrust uplifts the area south of the Shargyn Fault. The thrust is visible as a small, potentially recent [Bayasgalan et al., 2005], scarp in the alluvium. The Shargyn Fault marks a major lithologic change in this area. To the south of the Shargyn

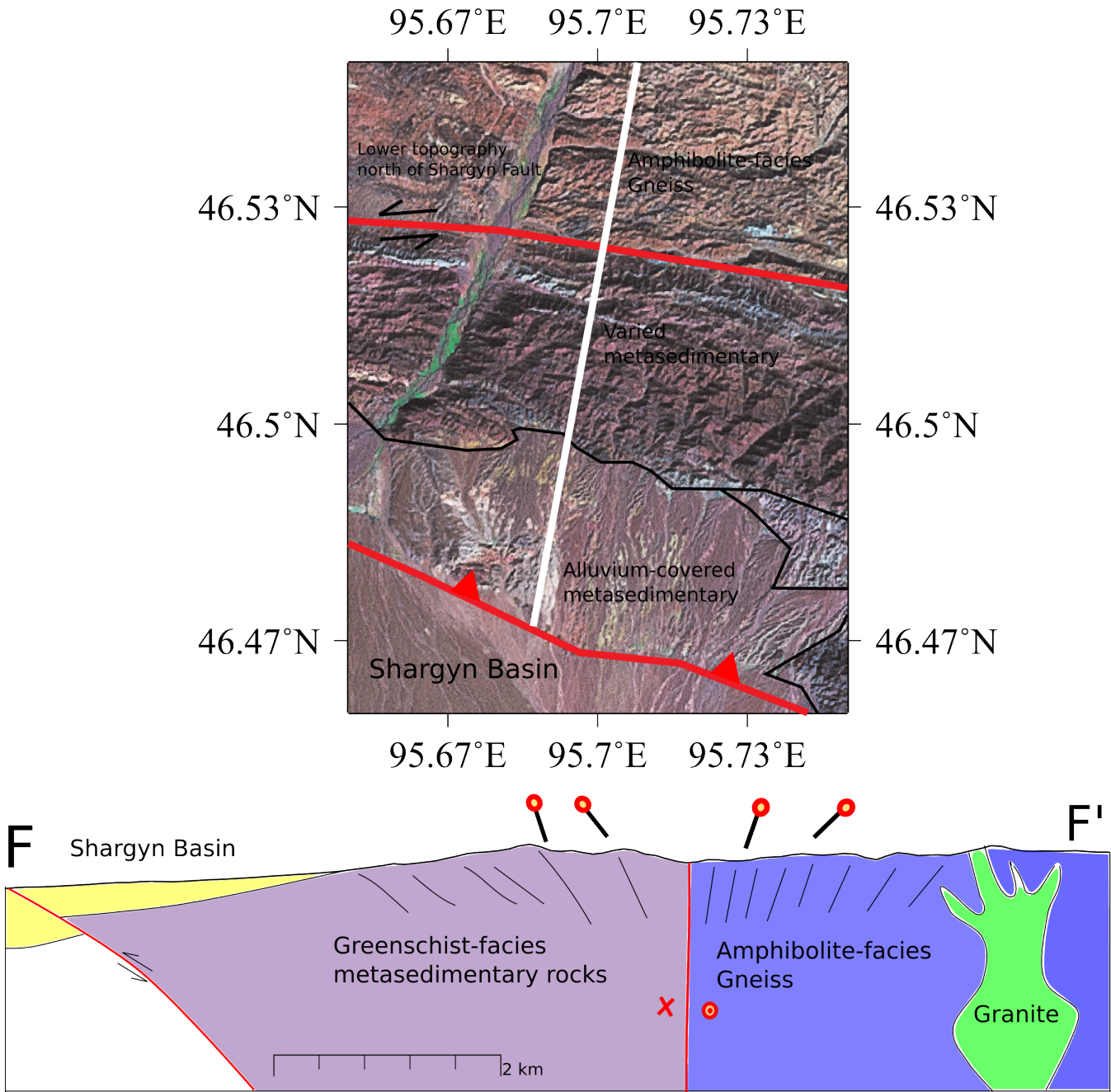


Figure 13: A cross-section through the Shargyn Fault in the northeast corner of the Shargyn Basin paired with a Landsat image of the surrounding area. Important locations and lithology are noted on the satellite image.

Fault, we find quartz-rich greenschist, metabasalt and carbonate units with foliations dipping to the north. On the north side of the fault, there are amphibolite facies gneiss and schist units with south-dipping foliations. There are also some large granitoid intrusions. Outcrops of garnet schist confirm the higher metamorphic grade. To the west, offset stream beds shown in Figure 14 provide one of the clearest indications of the active slip sense.

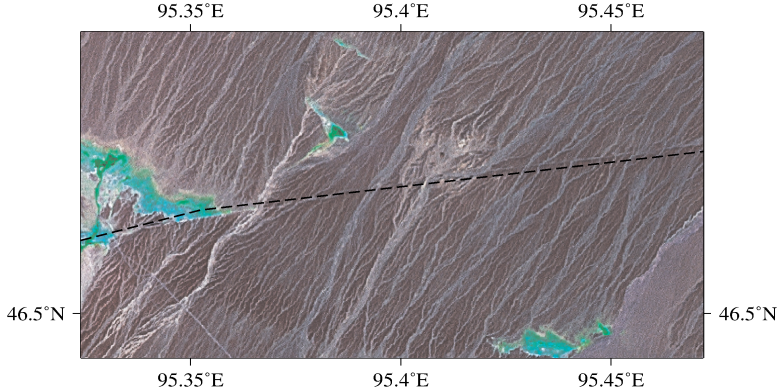


Figure 14: Offset stream beds along the ENE-WSW striking Shargyn Fault observed in Landsat imagery west of cross-section F-F'.

To the east, the strike of the Shargyn fault bends slightly southwards, at the cross-section marked X5-X5', shown in Appendix A. Here, the fault is still visible in satellite imagery as a eroded valley. To the south of the fault, we see steep rolling hills with highly deformed and metamorphosed amphibolite and gneiss. To the north of the fault, the topography is lower and transitions into alluvium. The northern unit is an slightly deformed alkali granite. The difference in metamorphic grade between the granite and the metamorphic unit indicates the granite was intruded after metamorphism. However, the contact between the granite and the metamorphic is perfectly straight, supporting the contact's interpretation as a fault. The topographic depression along the fault provides further evidence. To the east, the fault terminates somewhere near the city of Altai.

West of the transect, a thrust splay off the Shargyn Fault striking southwards. The thrust intersects the transect in the south between a red very poorly consolidated sandy unit and a steeply dipping shale. The northern side of the thrust is uplifted, while the basin is on the south side. Elevation profiles suggest there the fault accomodates increasing amounts of uplift further south. At its southern end, this thrust connects with the Upper Khantaishir Thrust.

### 3.7 Earthquake Mechanisms and Locations

Earthquake focal mechanisms provide useful information about active fault slip in the region. The available calculated focal mechanisms for western Mongolia are shown in Figure 2. The World Stress Map [Heidbach et al., 2009] uses focal mechanisms as the exclusive constraint on the primary stress axis in western Mongolia due to the lack of other data. Bayasgalan et al. [2005] provides a good review of the earthquake focal mechanisms in western Mongolia. Only a couple mechanisms are located in the Shargyn Basin. On the Shargyn Fault, near cross-section C-C', a focal mechanism

was calculated showing exclusively left-lateral slip. In the northern corner of the intersection wedge, a focal mechanism was calculated either showing low-angle south directed thrusting or high-angle north directed thrusting. Both possibilities are reasonable given the location of the earthquake.

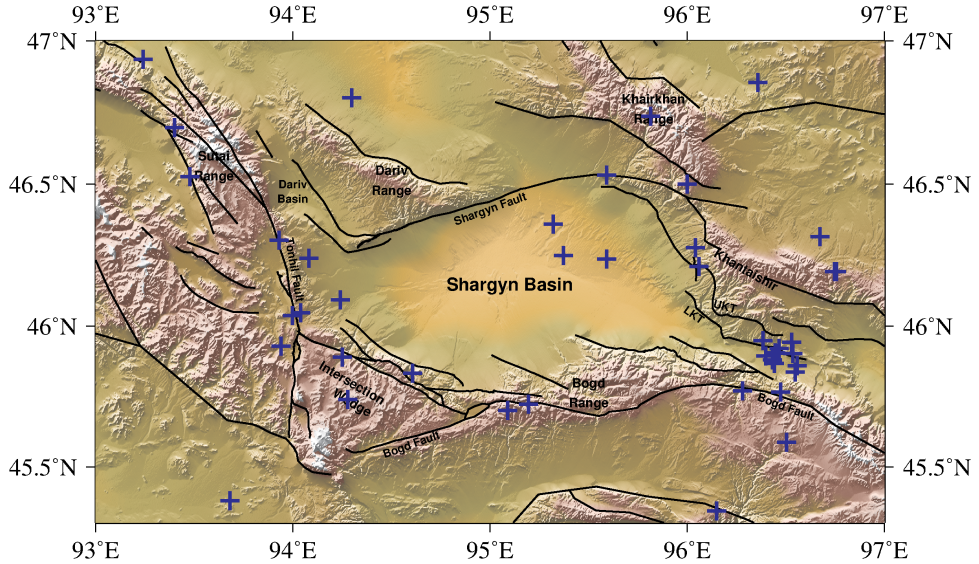


Figure 15: Shaded relief map of the Shargyn Basin showing blue plus signs where earthquakes have occurred between 1960 and 2013. Black lines are fault locations, like in Figure 7. Note that many of the earthquakes occur on, or near, mapped faults. However, three of the earthquakes occurred within the basin.

Earthquake locations can also constrain the location of active deformation. For smaller earthquakes, focal mechanisms cannot be calculated because there is a lack of data. However, locations can still be determined, albeit with significantly decreased accuracy. The locations for all the earthquakes available from the IRIS Data Management System in the Shargyn Basin region are shown in Figure 15. Most of these earthquakes occur around the margins of the basin at locations near where we have mapped faults. Notably, there are three earthquakes shown in the eastern part of the Shargyn Basin. We lack field or satellite data constraining the location of any fault through the basin here, so I did not map a fault. Furthermore, the error on some of the earthquake locations is large.

### 3.8 Interpretation and Discussion

The Shargyn Basin is a combination of a conjugate strike slip fault intersection and a left-lateral compressional strike-slip stepover. The Bogd Fault to the south, the Tonhil Fault to the west, the Shargyn Fault to the north and the Khantaishir Thrusts to the east are the primary faults governing the structure of the Shargyn Basin. The Bogd Fault and the Shargyn Fault are linked in a compressional stepover by the Khantaishir Thrusts. However, some motion remains on the continuation of the Bogd Fault. The remainder of this motion is transferred into multiple thrust splays, the last of which combines with terminal thrust splays from the Tonhil Fault to form an uplifted region that I will call the intersection wedge. Similar thrust splays on the Shargyn Fault uplift the Dariv Range and link with thrust faults in the Dariv Basin and the Sutai Range. Figure 16 shows a schematic diagram of this structure.

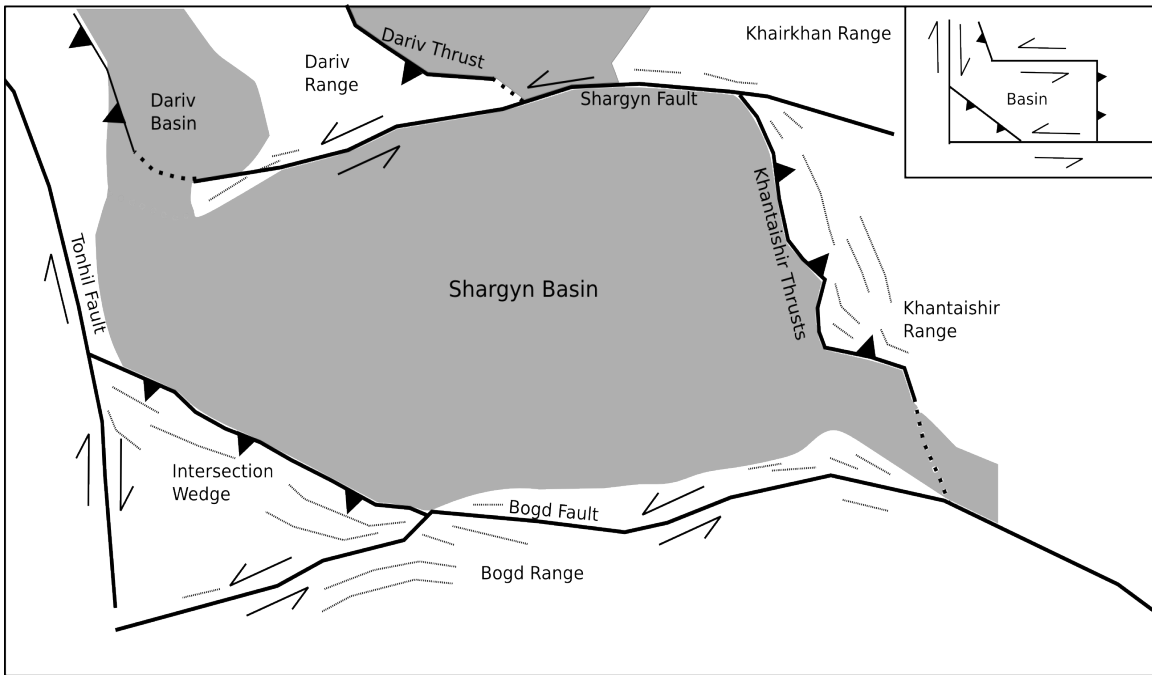


Figure 16: Schematic fault map of the Shargyn Basin region. The extent is approximately the same as the extent in Figure 3. Description of the structure is in the text. The shaded areas are basins. Unshaded areas are mountainous. The dotted lines represent the dominant foliation strike. The inset in the upper right is an even simpler description of the interacting stepover and wedge uplift.

Thus, the eastern part of the Shargyn Basin is a stepover basin forming from the Khantaishir Thrusts. The western and southern part of the basin is a foreland basin from the uplifted intersection wedge and the many termination thrust splays of the Bogd Fault. On the northern boundary, the uplift of the Dariv Range is concentrated on the Dariv Thrust and the Shargyn Fault separates the

low-lying basin from the adjacent mountain range while not accomodating the uplift.

Notably, the kinematics for the Shargyn Basin explain a large basin without any extension. Despite being deeper than most basins in the area (963m above sea level at the deepest), it would unexpected for the Shargyn Basin to have formed by any extensional process. Previous researchers have stated that the region has no normal faulting or transtensional faulting [Cunningham, 2005]. The low elevations do not require extension. The "Valley of the Lakes" to the north is at similar elevations. The small transtensional basins near the intersection wedge were the only extensional features we found. However, these transtensional basins are multiple orders of magnitude smaller than the Shargyn Basin. Further to the northeast, there are small normal faults linked by a major strike-slip fault [Walker et al., 2006]. These features are also much smaller than the Shargyn Basin.

With a kinematic description of the Shargyn Basin in hand, it is interesting to ask why such structures formed in their current locations. One answer to this questions involves pre-existing weaknesses in the crust. Near the stepover, the Bogd Fault bends southward 20-30 degrees. For most of its length, it closely follows the Main Mongolian Lineament. The Main Mongolian Lineament is probably a suture zone and separates a Late Proterozoic and Early Paleozoic orogeny on the north side from a Late Paleozoic orogeny on the south side. The bend in the Bogd Fault may be due to a bend in the Main Mongolian Lineament. Windley et al. [2007] has mapped the Main Mongolian Lineament as bending southwards in this area as well. On a broader scale, the Gobi-Altai and Altai ranges both follow the approximate structural grain in Figure 6.

In almost all (exluding specific parts of the intersection wedge) of the locations we studied the foliation strikes parallel or close to parallel to the important fault in the region. The foliations fit well with a model where faults form along structural weaknesses. The foliations could also be explained by dragging along the fault. With enough slip, regardless of the original foliation is an area, dragging of the foliation near the fault will lead to approximately fault-parallel strike. Dragging can be clearly seen in the satellite imagery of the beds along the Bogd Fault in the intersection wedge. However, in other locations, foliations are still fault-parallel 5-10km away from the surface trace of the fault and dragging is not seen. So, dragging may be locally important in the intersection wedge, but, elsewhere, it is more likely that the faults formed along pre-existing structural weaknesses.

## 4 Conclusion

The India-Eurasia collision causes deformation through a broad swath of Asia. In central Asia, the Altai Range and Gobi-Altai Range accomodate 10-15% of the total convergence rate [Calais, 2003]. Hence, western Mongolia has some of the best examples in the world of intracontinental deformation patterns. Here, we studied the zone where the Altai fault system and the Gobi-Altai fault system intersect. Transpressional strike-slip deformation is dominant and results in discrete fault block mountain ranges with small basins in between. The Shargyn Basin is an anomalously large basin for the region and begs explaining.

We describe the basin as a combination of two active structures. A left-lateral compressional stepover on the Bogd Fault forms the Khantaishir range and the Shargyn Fault. A conjugate strike-slip intersection between the Bogd Fault and the Tonhil Fault forms a wedge of uplifted material in the southwest corner of the basin. Further uplifts surround the basin due to termination thrust splays from the various strike-slip faults. Thus, the structure Shargyn Basin region is a prime example of the features that are common in intraplate transpressional orogenies and the part that pre-existing structural weaknesses can play in defining their locations.

# 1 Appendix A: More cross sections.

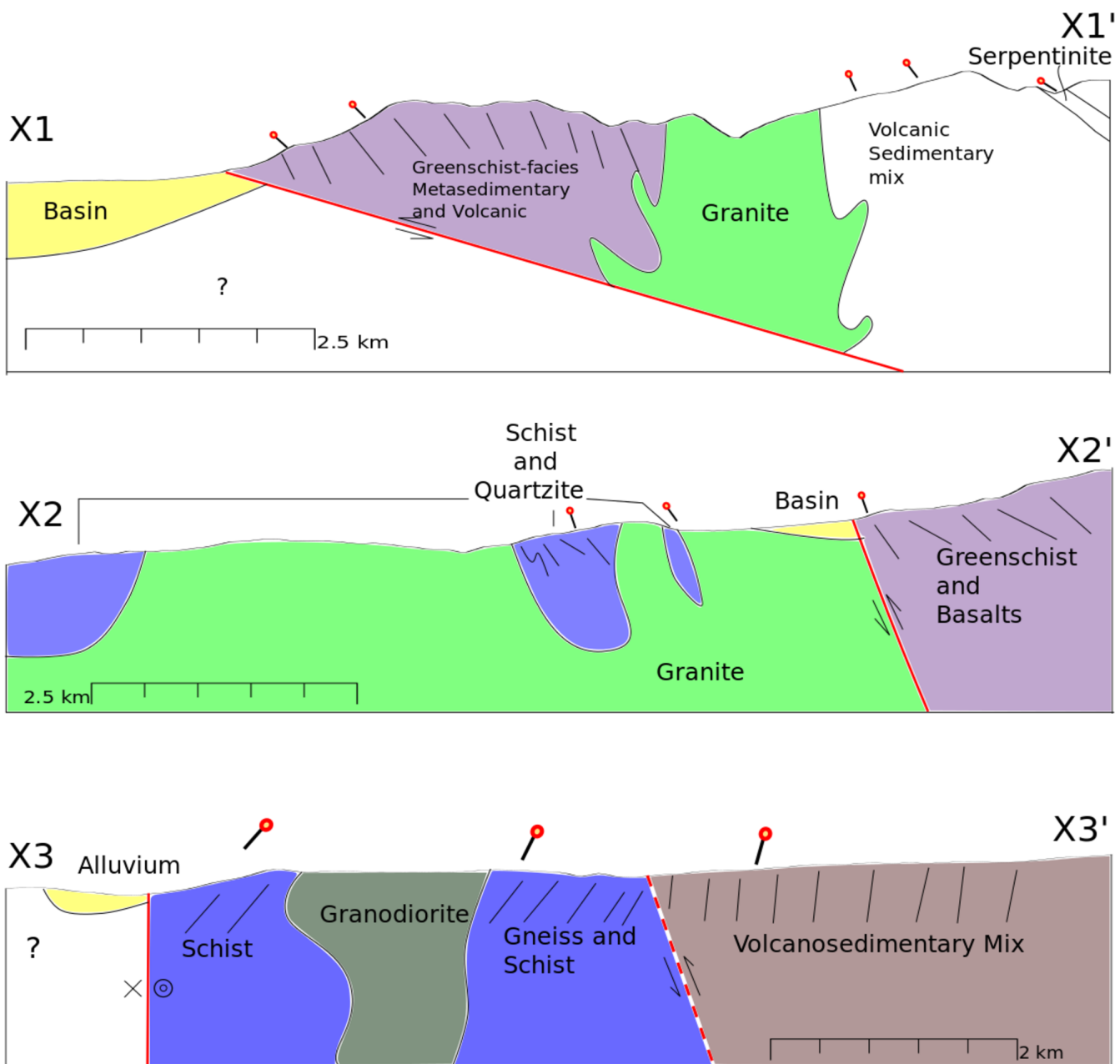


Figure 17: Cross section X1 across the Butara Thrust on the southern margin of the Shargyn Basin, cross section X2 across the final terminal thrust of the Bogd Fault, and cross section X3 examining the Tonhil Fault and northwestern corner of the intersection wedge.

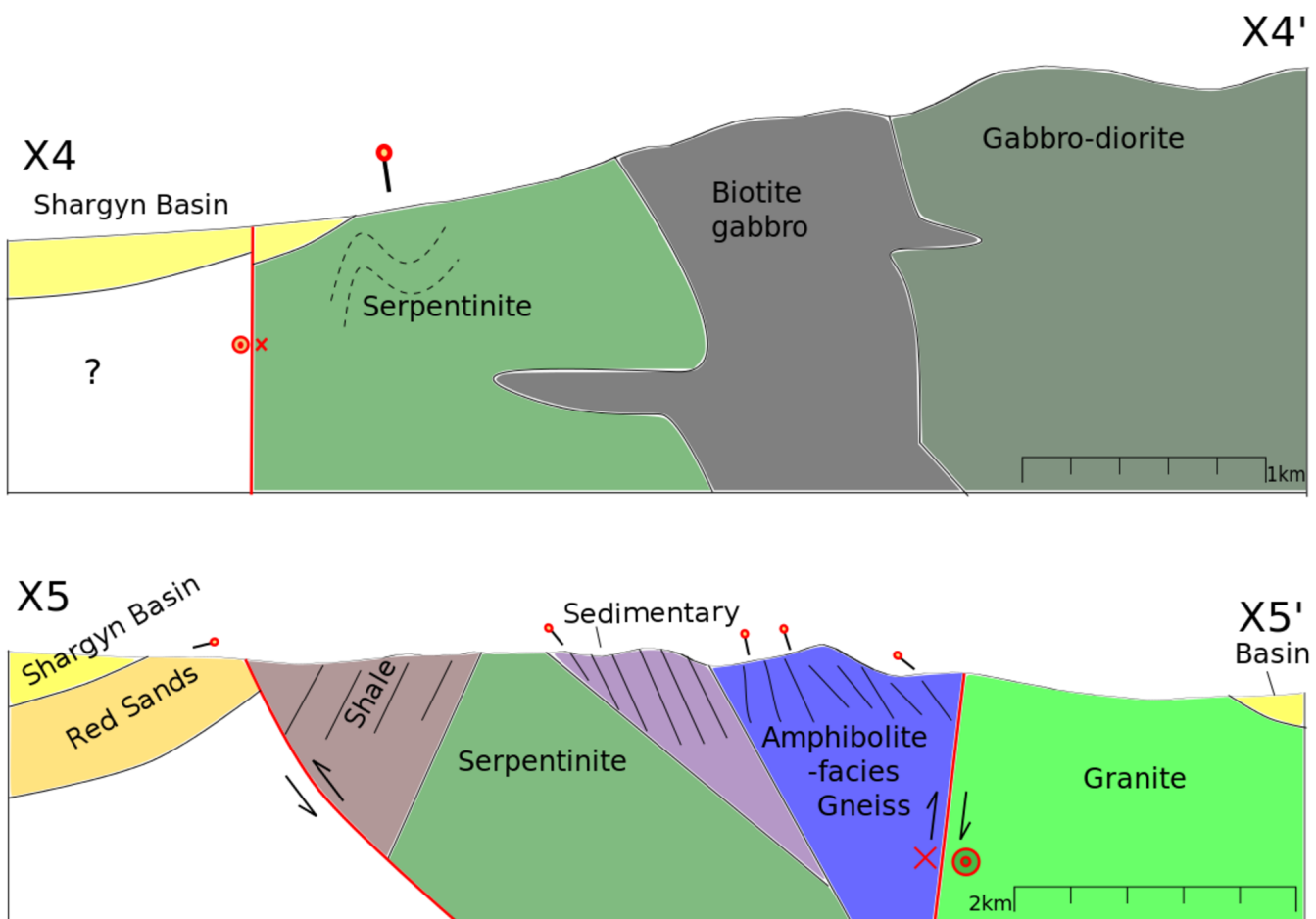


Figure 18: Cross section X4 through the Shargyn Fault at the southern margin of the Dariiv Range and cross section X5 at the eastern margin of the Shargyn Basin.

# Bibliography

C Bayarsayhan, A Bayasgalan, B Enhtuvshin, Kenneth W Hudnut, R A Kurushin, and Peter Molnar. 1957 Gobi-Altay , Mongolia , earthquake as a prototype for southern California's most devastating earthquake. *Geology*, 24:579–582, 1996. doi: 10.1130/0091-7613(1996)024j0579.

Amgalan Bayasgalan, James Jackson, and Dan McKenzie. Lithosphere rheology and active tectonics in Mongolia: relations between earthquake source parameters, gravity and GPS measurements. *Geophysical Journal International*, 163(3):1151–1179, December 2005. ISSN 0956540X. doi: 10.1111/j.1365-246X.2005.02764.x. URL <http://gji.oxfordjournals.org/cgi/doi/10.1111/j.1365-246X.2005.02764.x>.

C Busby and R Ingersoll. *Tectonics of sedimentary basins*. 1995. URL <http://bulletin.geoscienceworld.org/content/100/11/1704.short>.

Eric Calais. GPS measurements of crustal deformation in the Baikal-Mongolia area (1994-2002): Implications for current kinematics of Asia. *Journal of Geophysical Research*, 108(B10), 2003. ISSN 0148-0227. doi: 10.1029/2002JB002373. URL <http://www.agu.org/pubs/crossref/2003/2002JB002373.shtml>.

AR Carroll, L Yunhai, and SA Graham. Junggar basin, northwest China: trapped late Paleozoic ocean. *Tectonophysics*, 1990. URL <http://www.sciencedirect.com/science/article/pii/004019519090004R>.

PA Cowie and CH Scholz. Displacement-length scaling relationship for faults: data synthesis and discussion. *Journal of Structural Geology*, 14(10):1149–1156, 1992. URL <http://www.sciencedirect.com/science/article/pii/0191814192900666>.

D Cunningham. Active intracontinental transpressional mountain building in the Mongolian Altai: Defining a new class of orogen. *Earth and Planetary Science Letters*, 240

(2):436–444, December 2005. ISSN 0012821X. doi: 10.1016/j.epsl.2005.09.013. URL <http://linkinghub.elsevier.com/retrieve/pii/S0012821X05005881>.

D. Cunningham. Tectonic setting and structural evolution of the Late Cenozoic Gobi Altai orogen. *Geological Society, London, Special Publications*, 338(1):361–387, September 2010. ISSN 0305-8719. doi: 10.1144/SP338.17. URL <http://sp.lyellcollection.org/cgi/doi/10.1144/SP338.17>.

D Cunningham and LA Owen. Structural framework of a major intracontinental orogenic termination zone: the easternmost Tien Shan, China. *Journal of the ...*, 160:575–590, 2003. URL <http://jgs.lyellcollection.org/content/160/4/575.short>.

Dickson Cunningham, Sarah Davies, and Gombosuren Badarch. Crustal architecture and active growth of the Sutai Range, western Mongolia: a major intracontinental, intraplate restraining bend. *Journal of Geodynamics*, 36(1-2):169–191, August 2003. ISSN 02643707. doi: 10.1016/S0264-3707(03)00046-2. URL <http://linkinghub.elsevier.com/retrieve/pii/S0264370703000462>.

P Davy and PR Cobbold. Indentation tectonics in nature and experiment. 1. Experiments scaled for gravity. *Bull. Geol. Inst. Uppsala*, 1988. URL [http://blogperso.univ-rennes1.fr/philippe.davy/public/pdf/Davy\\_Cobbold\\_Bull.Uppsala\\_1988.pdf](http://blogperso.univ-rennes1.fr/philippe.davy/public/pdf/Davy_Cobbold_Bull.Uppsala_1988.pdf)

AH Dijkstra and FM Brouwer. Late Neoproterozoic proto-arc ocean crust in the Dariv Range, Western Mongolia: a supra-subduction zone end-member ophiolite. *Journal of the Geological Society, London*, 163:363–373, 2006. URL <http://jgs.geoscienceworld.org/content/163/2/363.short>.

P. England and P. Molnar. Active Deformation of Asia: From Kinematics to Dynamics. *Science*, 278(5338):647–650, October 1997. ISSN 00368075. doi: 10.1126/science.278.5338.647. URL <http://www.sciencemag.org/cgi/doi/10.1126/science.278.5338.647>.

Kurt L. Frankel, Karl W. Wegmann, Amgalan Bayasgalan, Robert J. Carson, Nicholas E. Bader, Tsolmon Adiya, Erdenebat Bolor, Chelsea C. Durfey, Jargal Otgonkhuu, Jodi Sprajcar, Kristin E. Sweeney, Richard T. Walker, Tina L. Marstellar, and Laura Gregory. Late Pleistocene slip rate of the Höh Serh-Tsagaan Salaa fault system, Mongolian Altai and intracontinental deformation in central Asia. *Geophysical Journal International*, 183(3):1134–

1150, December 2010. ISSN 0956540X. doi: 10.1111/j.1365-246X.2010.04826.x. URL <http://gji.oxfordjournals.org/cgi/doi/10.1111/j.1365-246X.2010.04826.x>.

Oliver Heidbach, Mark Tingay, Andreas Barth, John Reinecker, Daniel Kurfeß, and Birgit Müller. The World Stress Map based on the database release 2008, equatorial scale 1:46,000,000. *Commission for the Geological Map of the World*, 2009. doi: 10.1594/GFZ.WSM.Map2009.

G Houseman and Philip England. Crustal thickening versus lateral expulsion in the Indian Asian continental collision. *Journal of Geophysical Research*, 98(93), 1993. URL <http://onlinelibrary.wiley.com/doi/10.1029/93JB00443/full>.

JP Howard and WD Cunningham. Competing processes of clastic deposition and compartmentalized inversion in an actively evolving transpressional basin, western Mongolia. *Journal of the Geological Society, London*, 163:657–670, 2006. URL <http://jgs.lyellcollection.org/content/163/4/657.short>.

RA Kurushin, A Bayasgalan, M Olziybat, B Enhtuvshin, Peter Molnar, C Bayarsayhan, Kenneth W Hudnut, and Jian Lin. The surface rupture of the 1957 Gobi-Altay, Mongolia, earthquake. *Geological Society of American Special Paper*, 320:1–144, 1998. doi: 10.1130/0-8137-2320-5.1. URL <http://geology.gsapubs.org/content/24/7/579.short> <http://specialpapers.gsapubs.org/content/320/1.abstract>.

CJ Northrup, LH Royden, and BC Burchfiel. Motion of the Pacific plate relative to Eurasia and its potential relation to Cenozoic extension along the eastern margin of Eurasia. *Geology*, 1995. doi: 10.1130/0091-7613(1995)023;0719. URL <http://geology.gsapubs.org/content/23/8/719.short>.

Emile a. Okal. A surface-wave investigation of the rupture mechanism of the Gobi-Altai (December 4, 1957) earthquake. *Physics of the Earth and Planetary Interiors*, 12(4): 319–328, September 1976. ISSN 00319201. doi: 10.1016/0031-9201(76)90027-3. URL <http://linkinghub.elsevier.com/retrieve/pii/0031920176900273>.

Gilles Peltzer and F Saucier. Present-day kinematics of Asia derived from geologic fault rates. *Journal of Geophysical Research: Solid ...*, 10, 1996. URL <http://onlinelibrary.wiley.com/doi/10.1029/96JB02698/full>.

Fred Pollitz. Fault interaction and stress triggering of twentieth century earthquakes in Mongolia. *Journal of Geophysical Research*, 108(B10):2503, 2003. ISSN 0148-0227. doi: 10.1029/2002JB002375. URL <http://www.agu.org/pubs/crossref/2003/2002JB002375.shtml>.

W. Schellart and G. Lister. The role of the East Asian active margin in widespread extensional and strike-slip deformation in East Asia. *Journal of the Geological Society, London*, 162:959–972, 2005. URL <http://jgs.geoscienceworld.org/content/162/6/959.short>.

W.P. Schellart. Influence of the subducting plate velocity on the geometry of the slab and migration of the subduction hinge. *Earth and Planetary Science Letters*, 231(3-4):197–219, March 2005. ISSN 0012821X. doi: 10.1016/j.epsl.2004.12.019. URL <http://linkinghub.elsevier.com/retrieve/pii/S0012821X0400737X>.

P Tapponnier and P Molnar. Active faulting and Cenozoic tectonics of the Tien Shan, Mongolia, and Baykal regions. *Journal of Geophysical Research*, 84(9), 1979. URL <http://onlinelibrary.wiley.com/doi/10.1029/JB084iB07p03425/full>.

P Tapponnier, G Peltzer, and AY Le Dain. Propagating extrusion tectonics in Asia: New insights from simple experiments with plasticine. *Geology*, 10:611–616, 1982. URL <http://geology.geoscienceworld.org/content/10/12/611.short>.

R. T. Walker, E. Molor, M. Fox, and a. Bayasgalan. Active tectonics of an apparently aseismic region: distributed active strike-slip faulting in the Hangay Mountains of central Mongolia. *Geophysical Journal International*, 174(3):1121–1137, September 2008. ISSN 0956540X. doi: 10.1111/j.1365-246X.2008.03874.x. URL <http://doi.wiley.com/10.1111/j.1365-246X.2008.03874.x>.

R.T. Walker, a. Bayasgalan, R. Carson, R. Hazlett, L. McCarthy, J. Mischler, E. Molor, P. Sarantsetseg, L. Smith, B. Tsogtbadrakh, and G. Tsolmon. Geomorphology and structure of the Jid right-lateral strike-slip fault in the Mongolian Altay mountains. *Journal of Structural Geology*, 28(9):1607–1622, September 2006. ISSN 01918141. doi: 10.1016/j.jsg.2006.04.007. URL <http://linkinghub.elsevier.com/retrieve/pii/S0191814106001179>.

R.T. Walker, E. Nissen, E. Molor, and a. Bayasgalan. Reinterpretation of the active faulting in

central Mongolia. *Geology*, 35(8):759, 2007. ISSN 0091-7613. doi: 10.1130/G23716A.1. URL <http://geology.gsapubs.org/cgi/doi/10.1130/G23716A.1>.

BF Windley, D Alexeiev, and W Xiao. Tectonic models for accretion of the Central Asian Orogenic Belt. *Journal of the Geological Society, London*, 164(2004):31–47, 2007. URL <http://jgs.geoscienceworld.org/content/164/1/31.short>.

An Yin. Cenozoic tectonic evolution of Asia: A preliminary synthesis. *Tectonophysics*, 488(1-4):293–325, June 2010. ISSN 00401951. doi: 10.1016/j.tecto.2009.06.002. URL <http://linkinghub.elsevier.com/retrieve/pii/S0040195109003217>.